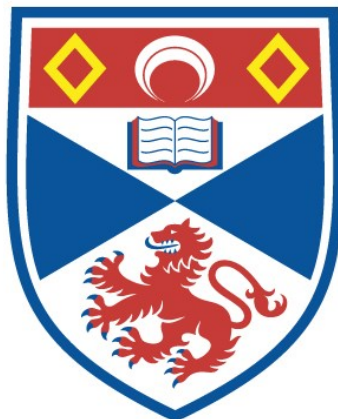


NUCLEAR MAGNETIC RESONANCE IN SOME  
HYDROCARBONS AT LOW TEMPERATURES

Ian James Lawrenson

A Thesis Submitted for the Degree of PhD  
at the  
University of St Andrews



1958

Full metadata for this item is available in  
St Andrews Research Repository  
at:

<http://research-repository.st-andrews.ac.uk/>

Please use this identifier to cite or link to this item:

<http://hdl.handle.net/10023/14615>

This item is protected by original copyright

NUCLEAR MAGNETIC RESONANCE

IN SOME HYDROCARBONS

AT LOW TEMPERATURES.

A Thesis

presented by

Ian J. Lawrenson, B.Sc.

to the

University of St. Andrews

in application for the Degree

of Doctor of Philosophy

ProQuest Number: 10171155

All rights reserved

INFORMATION TO ALL USERS

The quality of this reproduction is dependent upon the quality of the copy submitted.

In the unlikely event that the author did not send a complete manuscript and there are missing pages, these will be noted. Also, if material had to be removed, a note will indicate the deletion.



ProQuest 10171155

Published by ProQuest LLC (2017). Copyright of the Dissertation is held by the Author.

All rights reserved.

This work is protected against unauthorized copying under Title 17, United States Code  
Microform Edition © ProQuest LLC.

ProQuest LLC.  
789 East Eisenhower Parkway  
P.O. Box 1346  
Ann Arbor, MI 48106 – 1346

ms  
1989



DECLARATION

I hereby certify that this thesis has been composed by me, is a record of work done by me, and has not previously been presented for a Higher Degree.

The research was carried out in the Physical Laboratory of St. Salvator's College, in the University of St. Andrews, under the supervision of Dr. F. A. Rushworth.

CERTIFICATE

I certify that Ian J. Lawrenson, B.Sc., has spent nine terms at research work in the Physical Laboratory of St. Salvator's College, University of St. Andrews, under my direction, that he has fulfilled the conditions of Ordinance No. 16 (St. Andrews) and that he is qualified to submit the accompanying Thesis in application for the Degree of Doctor of Philosophy.

Research Supervisor.

### CAREER

I first matriculated in the University of St. Andrews in October 1951. I subsequently studied Mathematics and Natural Philosophy, and obtained the degree of Bachelor of Science with First Class Honours in Natural Philosophy in July 1955.

Following the award of a Scholarship in Electricity by Sir James Caird's Travelling Scholarships Trust, I commenced in August 1955 the work reported in this Thesis.

# C O N T E N T S

<u>Section</u>	<u>Page</u>
1. Introduction *** **	1
2. <u>Theory of Nuclear Magnetic Resonance</u>	
2.1 General Theory *** **	3
2.2 The Absorption Spectrum *** **	7
2.3 The Spin-Lattice Relaxation Process *** **	14
3. <u>Experimental Methods and Apparatus</u>	
3.1 General Requirements *** **	19
3.2 Bridge Method *** **	20
3.3 Spectrometer Method *** **	28
3.4 Cooling Systems *** **	35
4. <u>Experimental Results</u>	
4.1 Choice of Subjects for Study *** **	40
4.2 Cyclopentene *** **	43
4.3 n-Pentane and n-Hexane *** **	57
4.4 n-Octane *** **	59
4.5 Cyclooctatetraene *** **	80
5. <u>Summary</u> *** **	100
6. <u>References</u> *** **	102

1. INTRODUCTION

1. Introduction

The property of possessing an angular momentum, or spin, and an associated magnetic moment, was first attributed to the nucleus by Pauli (1924) to explain the hyperfine structure of atomic spectral lines.

Rabi and his co-workers (Rabi, Millman, Kusch and Zacharias 1939) achieved the first successful nuclear magnetic resonance experiments by applying the resonance principle to the atomic beam experiments of Stern and Gerlach. Transitions were produced between the quantised energy levels of the nucleus, by a process of stimulated emission or absorption.

It had been shown earlier (Gorter 1936) that similar effects should be observable in bulk matter: Gorter attempted unsuccessfully to detect absorption of energy by the  ${}^7\text{Li}$  nuclei in lithium fluoride, and by the protons in potassium alum, using a calorimetric method. Gorter and Broer (1942) tried, again unsuccessfully, to observe the resonance of  ${}^7\text{Li}$  and  ${}^{19}\text{F}$ .

The first successful experiments on nuclear resonance in bulk

matter were carried out independently by Purcell, Torrey and Pound (1946), and by Bloch, Hansen and Packard (1946). The first group used the technique now known as nuclear magnetic resonance absorption, which is the method employed here; the second group detected the resonance by the fundamentally similar method of nuclear induction.

Since 1946, nuclear resonance has been widely applied in many branches of physics. The most obvious application is to the accurate measurement of nuclear properties; conversely, if the nuclear gyromagnetic ratio is known, nuclear resonance provides a most accurate method of measurement of magnetic fields. However, some of the most interesting applications have been in the field of solid state physics: nuclear resonance can yield information on crystal and molecular structures, on hindered rotations of molecules and on thermal relaxation effects. It is with these applications that this thesis is concerned.

2. THEORY OF NUCLEAR MAGNETIC RESONANCE.



## 2.1. General Theory

The majority of nuclei possess a non-zero angular momentum, or spin, and an associated magnetic moment. If  $I$  is the nuclear spin number, then  $I\hbar$  is the maximum measurable angular momentum, where  $\hbar$  is Planck's constant divided by  $2\pi$ ;  $\mu$  is the maximum measurable component of the magnetic moment, and is related to the angular momentum by the relation  $\mu = \gamma I\hbar$ ,  $\gamma$  being the gyromagnetic ratio. Placing a non-interacting system of such nuclei in a magnetic field  $H_0$  removes the  $2I+1$  fold degeneracy, and the energy levels of the nucleus are given by  $-m\mu H_0/I$ , where  $m$  can take any integral values between  $+I$  and  $-I$ . Thus there are  $(2I+1)$  energy levels, separated by  $\mu H_0/I$ . This energy separation is often written as  $g\mu_0 H_0$ , where  $\mu_0$  is the nuclear magneton, and  $g$  ( $=\mu/\mu_0 I$ ) is the  $g$ -factor.

Transitions may then occur between these energy levels subject to the condition that  $m$  changes by  $\pm 1$ , corresponding to absorption or emission of energy. Therefore, a quantum of energy can produce

a transition between two levels if

$$h\nu_0 = \mu H_0 / I \quad (1)$$

where  $\nu_0$  is the frequency of the radiation applied. The nucleus at resonance in the experiments reported here is the proton: for this nucleus  $I = \frac{1}{2}$ , giving two energy levels of separation  $2\mu H_0$ , correspondingly roughly to alignment of the spin parallel or anti-parallel to the field. For the proton, equation (1) becomes

$$h\nu_0 = 2\mu H_0 \quad (2)$$

which is the fundamental resonance equation. For a field of 5000 gauss, a frequency of 21.5 Mc/s is required to produce transitions between the energy levels of the proton. The radiation must be circularly polarised with the magnetic vector rotating in a plane perpendicular to the magnetic field. This may be shown most easily by a classical representation. If the magnetic moment makes an angle  $\theta$  with the direction of the magnetic field, then the moment will precess around the field direction at the Larmor frequency. A radio frequency field perpendicular to

the steady field will tend to increase the angle  $\theta$ ; if the radio-frequency field is rotating around the steady field vector at the same rate as the magnetic moment, and in the same sense,  $\theta$  will increase steadily. Resonance thus occurs when  $\omega_0 = \gamma H_0$  where  $\omega_0$  is the Larmor angular frequency, this being exactly the same equation as (1). It is much easier in practice, however, to produce a linearly oscillating field; this is in general quite adequate, as it may be shown that a linearly oscillating field may be regarded as the superposition of two fields, rotating in opposite senses, only one of which has the correct sense to produce transitions, the other having a negligible effect.

Equation (2) applies also to the case of stimulated emission, the nuclei returning to the lower of the two energy states. Since the probabilities for emission and absorption are equal, a net absorption of energy will occur only when there is a surplus of spins in the lower state. This will be the case provided there is some mechanism ensuring that the spins are in temperature equilibrium with the lattice, when there will be a Boltzmann distribution between

the two states. For protons in a typical field of 5000 gauss, at room temperature, the ratio of the numbers of protons in the lower to the upper state is equal to  $\exp(2\mu H_0/kT) = 1 + 4 \times 10^{-6}$ . This very small excess of population in the lower state ensures a net absorption of energy from the radiofrequency field.

The mechanism keeping the spins at the same temperature as the lattice is known as the "spin-lattice relaxation process"; it has a characteristic relaxation time  $T_1$ , which is a measure of the efficiency of the process. The establishment of equilibrium is governed by the equation

$$n = n_0 \left(1 - \exp \frac{-t}{T_1}\right) \quad (3)$$

where  $n$  is the difference in population at time  $t$ , and  $n_0$  is the equilibrium value of this difference. A net absorption of energy will continue as long as the relaxation mechanism can maintain the population difference at its equilibrium value, despite the action of the electromagnetic field, causing transitions to the higher level. If too great an electromagnetic field is applied, the relaxation mechanism will be unable to cope; the absorption will

decrease, and the specimen is said to be saturated.

## 2.2 The Absorption Spectrum

The equation  $h\nu_0 = 2\mu H_0$  applies only to an isolated proton, or to the hypothetical case of a system of non-interacting spins. The protons in a solid, however, are not isolated, but are surrounded by a large number of other protons, each with a magnetic moment  $\mu$ . Therefore, each proton finds itself in a field  $H_0 + H_{\text{local}}$ , where  $H_0$  is the steady field, and  $H_{\text{local}}$  is the instantaneous sum of the magnetic fields produced by the neighbouring protons. Only nearest neighbours are important, since the magnetic field of a dipole of magnetic moment  $\mu$  at a distance  $r$  is of the order of  $\mu/r^3$ . Taking  $r$  equal to 1 Å, and  $\mu$  one nuclear magneton, we obtain  $H_{\text{local}}$  equal to approximately 5 gauss: the value of the local field, therefore, is typically a few gauss.

For a system of interacting protons, therefore, the resonance condition becomes

$$h\nu_0 = 2\mu(H_0 + H_{\text{local}}) \quad (4)$$

and the resonance spectrum is broadened to a few gauss.

The actual value of  $H_{\text{local}}$  depends on the arrangement of the protons in the molecule, and in the crystal lattice. It is theoretically possible, therefore, to calculate the absorption spectrum expected for a given proton configuration. In those cases where the protons are in close groups of 2, 3 or 4 molecules, detailed perturbation calculations have been made. Pake (1948) analysed the spectrum obtained from gypsum,  $\text{CaSO}_4 \cdot 2\text{H}_2\text{O}$ , in which the protons are in pairs, with next nearest neighbours considerably farther distant. The spectrum expected for a system of three protons situated at the corners of an equilateral triangle has been calculated by Andrew and Bersohn (1950), and for protons at the corners of an isosceles triangle by Andrew and Finch (1957). The spectrum resulting from groups of four protons has been calculated only in certain special cases.

For more complicated cases, perturbation calculations are not suitable, and the line shape cannot be predicted. However, Van Vleck (1948) has shown that the moments of the spectrum can be



calculated. The "second moment" is defined as the mean value of the square of the frequency deviation from the centre of the resonance, the average being taken over the line-shape function.

Thus if  $\nu_0$  is the resonant frequency, the second moment is

$$\langle (\Delta\nu)^2 \rangle_{av} = \int_{-\infty}^{\infty} (\nu - \nu_0)^2 g(\nu) d\nu \quad (5)$$

The line shape function  $g(\nu)$  is normalised,

i.e. 
$$\int_{-\infty}^{\infty} g(\nu) d\nu = 1$$

and so 
$$\langle (\Delta\nu)^2 \rangle_{av} = \frac{\int_{-\infty}^{\infty} (\Delta\nu)^2 g(\nu) d\nu}{\int_{-\infty}^{\infty} g(\nu) d\nu}$$

$$= \frac{\left[ g(\nu) \frac{(\Delta\nu)^3}{3} \right]_{-\infty}^{\infty} - \frac{1}{3} \int_{-\infty}^{\infty} (\Delta\nu)^3 \frac{dg(\nu)}{d\nu} d\nu}{\int_{-\infty}^{\infty} g(\nu) d\nu}$$

$g(\nu)$  vanishes except when  $\nu$  is very nearly equal to  $\nu_0$ , and

therefore

$$\langle (\Delta\nu)^2 \rangle_{av} = \frac{-\frac{1}{3} \int_{-\infty}^{\infty} (\Delta\nu)^3 \frac{dg(\nu)}{d\nu} d\nu}{\int_{-\infty}^{\infty} g(\nu) d\nu}$$

In practice it is usually more convenient to vary the magnetic field,

$H$ , keeping the frequency constant. If  $h = H - H_0$ , then the second

moment can be written as

$$\langle (\Delta H)^2 \rangle_{av} = \frac{\frac{1}{3} \int h^3 \frac{df(h)}{dh} dh}{\int h \frac{df(h)}{dh} dh} \quad (6)$$

where  $f(h)$  is the line shape function expressed as a function of the magnetic field.

For the second moment expressed in gauss<sup>2</sup>, Van Vleck's theory gives the expression

$$\text{Second Moment} = \frac{3I(I+1)}{2N_r} g^2 \sum_{j>k} (3\cos^2\theta_{jk} - 1)^2 r_{jk}^{-6} + \frac{1}{3} \frac{\mu_0^2}{N_r} \sum_i \sum_f I_i(I_i+1) g_i^2 (3\cos^2\theta_{if} - 1)^2 r_{if}^{-6} \quad (7)$$

where  $g$ ,  $I$  are the nuclear  $g$ -factor and spin of the nucleus at resonance,

$g_f$ ,  $I_f$  are the nuclear  $g$ -factor and spin of the other nuclei present,

$r_{jk}$  is the length of the vector connecting nuclei  $j$  and  $k$ ,

$N_r$  is the number of nuclei at resonance which are present in the system whose interactions are considered, and over which the sum is taken.

For a polycrystalline specimen,  $(3\cos^2\theta - 1)^2$  has to be averaged over a sphere; also, all the samples examined in this thesis have only one species of nucleus with a magnetic moment. Thus:



Second Moment of  
Polycrystalline Sample

$$= \frac{6}{5} \frac{I(I+1)}{N_R} g^2 \mu_0^2 \sum_{j k} r_{jk}^{-6} \text{ gauss}^2$$

Inserting the values given by Bearden and Watts (1951), we obtain finally

$$\text{Second moment} = \frac{715.9}{N_R} \sum_{j k} r_{jk}^{-6} \text{ gauss}^2. \quad (8)$$

This equation for the second moment assumes that the protons are at rest. Any motion of the protons will tend to average out the interactions and thus reduces the width of the absorption spectrum. The effect of molecular motion was investigated by Gutowsky and Pake (1950). They introduced a correlation frequency  $\nu_c$ , which describes the average rate at which significant changes occur in the atomic arrangement around the nucleus, and obtained

$$(\delta\nu)^2 = A^2 \left(\frac{2}{\pi}\right) \tan^{-1} \left[ \alpha \frac{\delta\nu}{\nu_c} \right]. \quad (9)$$

where  $\delta\nu$  is the line-width expressed as a frequency, and  $\alpha$  is a constant of the order of unity. As  $\nu_c \rightarrow 0$ , then  $\delta\nu \rightarrow A$ , the rigid lattice line-width; as  $\nu_c$  increases to the value  $A$ , the line-width  $\delta\nu$  decreases. The line will be in the process of broadening when  $\frac{\delta\nu}{\nu_c} \sim 1$ .  $A$  is typically of the order of 100 Kc/s, thus the resonance may be narrowed by relatively low-frequency motion.

Various forms of molecular motion may occur. These include rotation, quantum mechanical tunnelling through the potential barrier, if the axis of rotation is also a symmetry axis of the molecule, rotational oscillation, spinning about fixed centres of gravity, and diffusion of the molecules through the lattice. All these forms of motion will cause the resonance spectrum to narrow, provided the average frequency of motion exceeds the minimum reorientation frequency. The factor  $(3\cos^2\theta - 1)^2/r^3$  in equation (7) must be replaced by its average value over the motion, giving the theoretical value for the second moment with molecular motion.

This theory has been used successfully by many authors to correlate line-width changes with molecular motion. However, Anderson (1954) has shown that the second-moment should be invariant with respect to molecular motion.

The solution to this paradox lies in the fact that the local field  $H_{\text{local}}$  is not in fact constant, but varies with time (Andrew 1957). The frequency of precession of the nuclear magnet about the magnetic field can then be shown to be frequency-modulated, with a time-averaged

value equivalent to that for a steady local field. In the case of a pair of protons, rotating about an axis perpendicular to the interproton vector, and making an angle  $\alpha$  with the steady magnetic field, Van Vleck's theory shows that the absorption spectrum consists of two lines, with an angular frequency separation of  $\gamma \frac{3H}{2r^3} (3\cos^2\alpha - 1)$ . Considering the fluctuating local field, the spectrum can be shown to consist of the same two lines, plus the infinite set of side-bands associated with a frequency-modulated carrier wave. The amplitude of the  $n$ 'th side-band is given by the Bessel function  $J_n^2(m)$ , where  $m$  is the modulation index. The side-bands are thus very weak. In practice, the two protons never rotate at a constant frequency: the angular frequency can then be analysed into a set of frequencies, each frequency having its own set of side-bands. This reduces still further the intensity of the side bands.

It can be shown that the second moment, including the second moment of the side-bands, is equal to that obtained for a non-rotating pair of protons showing that the true second moment is indeed variant. However, the second moment normally measureable, that of the central portion of the spectrum, is reduced in accordance with Van Vleck's

theory, which can thus be used for the investigation of molecular motion.

### 2.3 The Spin-Lattice Relaxation Process

We have shown in section 2.1 the need for a mechanism keeping the spins at the same temperature as the lattice, thus ensuring a steady absorption of energy from the radio-frequency field. The nature of this mechanism will be discussed later; at present it is sufficient to assume that such a mechanism does exist, and that it originates in the thermal motion of the molecules. Such a mechanism is called the "spin-lattice relaxation process".

Suppose we have a system containing nuclei with  $I = \frac{1}{2}$ , such that the spin system and the lattice are in thermal equilibrium at some temperature  $T$ , and in a very weak magnetic field. The energy difference between the two levels will then be very small, and the populations, determined by the Boltzmann relation, will be almost equal. If this system is now transferred to a strong field  $H_0$ , the almost equal distribution of nuclei between the two levels will correspond to a very high spin temperature  $T_s$ . The spin system

will then try to attain a new distribution in thermal equilibrium with the lattice. It can be shown (Andrew 1955) that  $n$ , the population difference at time  $t$ , and  $n_0$ , the equilibrium difference, are related by the equation

$$n = n_0 (1 - e^{-t/T_1}) \quad (10)$$

Thus, the approach to equilibrium is exponential, with a characteristic time  $T_1$ , the "spin-lattice relaxation time".

Equation (10) may be written

$$\frac{dn}{dt} = \frac{n_0 - n}{T_1}$$

In the presence of radiation we must subtract a term from the right hand side of this equation to account for the upward transitions corresponding to the net absorption of energy. If  $P$  is the probability per unit time of a transition between the levels due to the radiation, then

$$\frac{dn}{dt} = \frac{n_0 - n}{T_1} - 2nP$$

since each transition changes  $n$  by 2. A steady state is reached when  $dn/dt = 0$ ; thus

$$\frac{n_s}{n_0} = \frac{1}{1 + 2PT_1} \quad (11)$$

$n_s$  being the steady state value of the population difference.

Hoenberger, Purcell and Pound (1948) have shown that the probability

P of a single transition is given by

$$\frac{1}{4} \gamma^2 H_1^2 g(\nu)$$

where  $\gamma$  is the gyromagnetic ratio,  $2h_1$  is the amplitude of the radio-frequency magnetic field, and  $g(\nu)$  is the normalised line-shape function.

Equation (11) may therefore be expressed as

$$\frac{n_s}{n_0} = \frac{1}{1 + \frac{1}{2} \gamma^2 H_1^2 T_1 g(\nu)} \quad (12)$$

We see, therefore that if the radio frequency field is too large,  $n_s/n_0$  becomes quite small: the absorption decreases and the specimen is saturated. The amount of saturation varies, being greatest at that frequency which gives  $g(\nu)$  its maximum value.

Since the line-shape function  $g(\nu)$  is normalised, its peak value will give an inverse measure of its width. It is customary, therefore, to define another relaxation time, the "spin-spin relaxation time" by the relation

$$T_2 = \frac{1}{g(\nu)_{\max}}$$

We then obtain, from equation (12)



$$\frac{n_B}{n_0} = \frac{1}{1 + \gamma^2 H_1^2 T_1 T_2} = Z_0 \quad (13)$$

at the maximum of the line-shape function,  $Z_0$  being known as the saturation factor.

Thus the maximum steady state absorption is experienced only when  $2H_1$ , the amplitude of the radiofrequency magnetic field producing transitions is such that  $\gamma^2 H_1^2 T_1 T_2 \ll 1$ . For larger values of  $H_1$ , the maximum absorption is reduced by the factor  $1/(1 + \gamma^2 H_1^2 T_1 T_2)$ .

This saturation effect provides a method of measuring  $T_1$ , and will be further discussed in section (4.4.5).

In the case of liquids, Bloembergen, Purcell and Pound (1948) showed that the most effective mechanism producing spin-lattice relaxation was the random translational and rotational motion of the molecules. Such motion produces rapidly fluctuating local fields at the nucleus. The component at the resonant frequency  $\nu_0$ , or at  $2\nu_0$ , of the Fourier spectrum of this fluctuation will cause transitions between energy levels.

For solids where molecular reorientation or translation is

occurring, a similar process will dominate the relaxation.

For rigid lattices, however, this will not apply. Waller (1932) and Heitler and Teller (1936) investigated the effect of thermal lattice vibrations, but concluded that this mechanism was not sufficiently powerful to give relaxation times in agreement with experimental values.

Rollin and Hatton (1948) and Bloembergen (1949) suggested that the paramagnetic impurities, always present in extremely small quantities, actually controlled the relaxation. The spin energy is then transferred to the lattice via the large electronic magnetic moment of the paramagnetic ion. This process does give relaxation times in fairly good agreement with experiment.



3. EXPERIMENTAL METHODS AND APPARATUS

### 3.1 General requirements

The main requirements for the detection of nuclear magnetic resonance absorption are a source of radiofrequency power at a frequency  $\nu_0$ , and a steady magnetic field  $H_0$ .  $\nu_0$  and  $H_0$  are then related by the resonance equation  $h\nu_0 = 2\mu H_0$ .

Bloembergen et al (1948) have shown that the signal-to-noise voltage obtained is proportional to  $\nu_0^{7/4}$ ; a higher field  $H_0$  not only increases the spacing between the levels,  $2\mu H_0$ , but also enhances the population ratio by the Boltzmann factor  $e^{2\mu H_0/kT}$ . It is advantageous, therefore, to operate at as high a frequency as possible. Practical limitations in the electronic equipment, however, make it advisable to use a frequency less than 30 Mc/s; the resonant frequency employed in the experiments reported here was 22.4 Mc/s, corresponding to a magnetic field strength of 5260 gauss.

Several experimental methods have been developed to detect the resonance absorption, two of which have been employed here, and will be described in detail. Both methods measure the resonance by its effect on a tuned radiofrequency coil containing the specimen. When

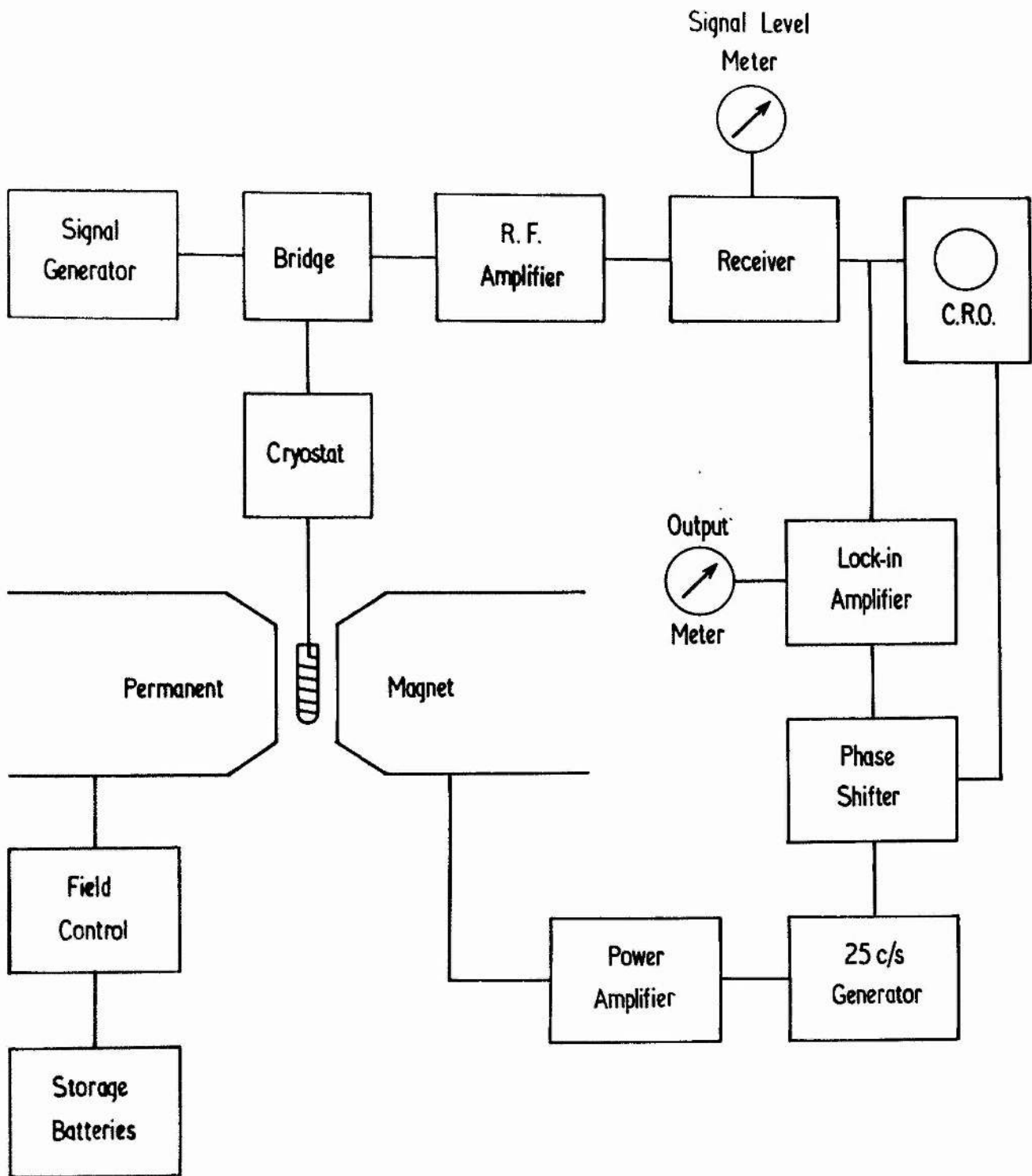


FIGURE 1

this coil is placed at right-angles to a steady magnetic field, then the absorption occurring at the resonant frequency is shown as a change in amplification factor  $Q$  of the coil.

### 3.2 Bridge method

This is the most widely-used method of detecting resonance absorption, and was employed in the first successful experiments of Purcell et al (1946). A more convenient arrangement was developed by Bloembergen et al (1948).

The apparatus required is indicated diagrammatically in figure 1. The specimen to be examined is held in a coil, at right-angles to the steady field  $H_0$ . When quanta of radiation at the appropriate resonant frequency  $\nu_0$  are supplied to the coil by a commercial Signal Generator, the conditions for resonance are obeyed, and absorption of energy takes place. The absorption is detected as additional power loss, equivalent to an extra resistance, in the coil; the  $Q$  of the coil changes. In order to display the resonance more clearly, the main magnetic field is modulated at 25 c/s with an amplitude of a few gauss, by means of auxiliary coils. Thus, the field is swept

through the resonant value twice in each cycle, giving an audio modulation of the carrier. This is then amplified and demodulated, and the resultant audio output fed to an oscillograph. If the X-plates of the oscillograph are supplied with a 25 c/s signal, phased correctly with respect to the current in the field modulation coils, the absorption line shape is displayed.

However, the depth of modulation produced is extremely small. A radiofrequency bridge is therefore introduced to the circuit, in order to balance out most of the carrier, and thus enhance the depth of modulation. A greater radiofrequency amplification before detection is then possible, making for a better signal-to-noise ratio. A further advantage is that any spurious noise produced by the signal generator is largely balanced out. However, this method permits both absorption and dispersion curves to be plotted. If the bridge is balanced in phase, but partially unbalanced in amplitude, the absorption curve is obtained; if balanced in amplitude but not in phase, the dispersion curve is obtained. By incorrect adjustment of the bridge, it is possible to observe a combination of the two curves, resulting in a distortion of the required absorption curve.

In this way narrow resonance lines have been observed. For solids, however, the line is usually several gauss broad, and the absorption intensity is correspondingly smaller. The strength of the signal obtained is often comparable with the noise present, and a display on an oscillograph is impossible. Such a display requires a reasonably broad bandwidth (about  $10^3$  c/s). An improvement in the signal-to-noise ratio would result from a reduction of this band-width, and this is achieved by the use of a "lock-in" amplifier, or phase-sensitive detector. When this unit is used, the field modulation is reduced to a fraction of the line-width, and the "steady" field slowly swept through the resonant value: the output, displayed on a recording meter, is proportional to the first derivative of the absorption line.

Some sections of the apparatus will now be described in detail, in order to emphasise the more important requirements.

(1) Permanent Magnet

The main advantage of a permanent over an electromagnet is the easily attained field stability. The magnet used in the experiments reported here, was designed by Andrew and Rushworth (1952), and

described fully by Rushworth (1955). The specifications are:

Field strength: 5260 gauss. Pole face diameter: 8 inches.

Gap width: 2 inches.

The pole-pieces are built up of 90° segments of Alcomax III, and the pole caps are of Armco iron. Specially designed ring shims are employed to increase the field homogeneity.

The original magnetising coils were retained, and are used to sweep the steady field. The necessary current for this is supplied by storage batteries, and a motor-driven potentiometer.

#### (ii) Signal Generator

An Airtec Signal Generator, Type 701, was used, giving an output between  $10^{-5}$  and 1 volt. It is most important that there is no frequency modulation of the output; accordingly the valves were heated by a D.C. supply, and a well-smoothed external H.T. unit was used, to eliminate 50 c/s ripple.

#### (iii) Radiofrequency Bridge

The twin-T bridge used here is similar to that described by Anderson (1949) (figure 4). An analysis of this circuit shows that



the controls for phase and amplitude balance are independent.

Because of the asymmetry of the bridge, it is very frequency-dependent, and any frequency modulation of the signal generator output must be avoided.

Normally the bridge is balanced in amplitude so that the carrier is reduced to between one and three per cent of the level being fed into the bridge (30 to 40 db balance).

#### (iv) Radiofrequency Amplifier

An Eddystone Communications Receiver, Type 680, provides most of the radiofrequency amplification, as well as the audio amplification and demodulation. Power supplies again come from external units. A meter shows the current flowing in the second detector valve, and thus gives an indication of the carrier level.

To avoid saturation of the sample at low temperatures, the radiofrequency voltage applied across the coil may have to be as low as 0.002 V; it is important, therefore to have optimum conditions, in order to obtain the best possible signal-to-noise ratio. For this reason, the receiver was preceded by a pre-amplifier.



The main pre-amplifier used has been described by Hades (1952). It is a single stage unit, employing a pentode, Mullard Type EF 54. Balanced input and output tuned circuits are used, being inductively coupled to the coaxial feeders.

The noise factor of the pre-amplifier was measured using a noise diode, type GEC A2087. The noise factor of an amplifier is defined as "the ratio of the actual noise power at the output terminals to that which it would have if the noise were limited to the minimum noise from thermal agitation" (Spangenberg 1948, p321). The noise factor of the entire radiofrequency amplifier is essentially that of the pre-amplifier alone, as it has a high gain and a narrow bandwidth. The method of measurement followed Moxon (1949, p74), who shows that the noise factor is given by

$$N_f = 20IR$$

where I is the diode anode current in amps which, flowing in a resistance R, doubles the total power indicated at the second detector. The noise factor for this amplifier was 2.5 db.

Another pre-amplifier, of the "cascode" type, was built, to try to improve even upon this noise factor. The "cascode" amplifier

(Wallman, MacNee and Gadsden, 1948) consists of a grounded-cathode triode followed by a grounded-grid triode. This arrangement combines the low noise factor of a triode with the high amplification and stability of a pentode. The valves used in the "cascode" were a triode-connected 6AK5 (grounded-cathode) and half of a 6J6 (grounded-grid), as recommended by Wallman et al. Two further stages of amplification were added: both employed 6AK5 valves and were tuned. Input and output were loosely coupled inductively; the input coupling was carefully adjusted to give optimum noise factor when connected to the output impedance of the bridge. The valves were heated by batteries, and the H.T. was supplied by a well-smoothed external unit.

The best noise factor obtained with this pre-amplifier was 2 db. However a slight "staggering" of the tuned circuits increased this figure considerably and, for general use, the single valve pre-amplifier was preferred. This was a much simpler circuit, and could very easily be kept exactly tuned by a single external tuning control.

(v) Lock-in Amplifier

This unit follows the circuit developed by Dicke (1946) and described by Bloembergen (1948).

To plot an absorption line shape, the field modulation is reduced to a fraction of the linewidth, and the steady field is slowly swept through the region where resonance absorption occurs. The resulting 25 c/s modulation of the R.F. carrier is amplified and detected and the audiofrequency output together with noise fed to the lock-in amplifier. The first stage of this unit is a narrow band 25 c/s amplifier, followed by a balanced stage where the input signal is mixed with a suitably phased 25 c/s reference voltage. The D.C. output of this stage depends upon both amplitude and phase of the input signal. Following the mixer stage is a D.C. amplifier leading to the output meter. The noise voltages, being random, are equally likely to affect the output in either direction; their resultant, therefore, tends to zero as the time constant of the R-C circuit connecting the mixer and D.C. amplifier stages is increased. A long time constant requires that the steady field be swept at a slow rate. Four values were incorporated in the circuit: 0.5, 3, 5 and 8 seconds, the shorter being for direct visual observation of the output meter, the longer for use with the recording micro-ammeter. This measuring technique indicates the first derivative of the absorption line shape.

(vi) Field Modulating Equipment

The 25 c/s generator consists of a multivibrator followed by a two-stage selective amplifier; this method enables the phase of the 25 c/s signal to be fixed relative to that of the mains voltage, and eliminates beat voltages in the output of the receiver. This generator supplies the 25 c/s reference signal required by the lock-in amplifier, and also the power amplifier leading to the modulation coils.

The power amplifier can deliver 25 watts at 25 c/s into the coils, which consist of 1000 turns of 22 swg wire wound on ebonite formers.

3.3 Spectrometer Method

The specimen is again held in a coil, perpendicular to the steady magnetic field. This coil, and a tuning condenser in parallel, form the grid-circuit of a radiofrequency oscillator. The normal circuit losses in an oscillator are replenished by the feedback, suitably phased, which may be described in terms of a negative resistance in parallel with the tuned circuit. When

the feedback energy tends to exceed the losses in the tank circuit, the level of oscillation increases, being limited by the curvature of the valve characteristics. Radiofrequency power flows in the specimen coil, and, if oscillations occur at the resonant frequency, nuclear resonance absorption will take place. This is equivalent to a change in the effective coil resistance, and shows up as a change in the level of oscillation. If the steady field is again modulated at 25 c/s, the resonance absorption produces an audio-frequency modulation of the resonant frequency carrier wave.

In operation it is advantageous to maintain oscillations at as low a level as possible, as the sensitivity is then greatest. The oscillator then has its optimum value for noise factor, as at higher levels the non-linearity of the characteristics introduces noise components originating in a wide band of frequencies. The main reason, however, is to avoid saturation of the specimen. It is not possible to reduce the radiofrequency amplitude across the coil much below 0.1V, which would cause saturation in most solids. This method, therefore, is used mostly with liquid specimens.

The circuit constructed followed closely that of Pound (1952).



The detector is separated from the oscillator by a two-stage radiofrequency amplifier, and leads to two stages of audiofrequency amplification. Automatic gain control keeps the level of oscillation steady. This spectrometer shows only the absorption line, although the dispersion may be detected as frequency modulation of the carrier.

This circuit may be used to search for resonances by sweeping the frequency. However, we are interested only in the resonance of protons, and so the oscillator is required to operate only in a restricted frequency range. The two R.F. amplifier stages were therefore tuned, to give a greater amplification before detection, and a better noise factor. Oscillations could be maintained at frequencies between 21.5 and 23.5 Mc/s, corresponding to field strengths lying between 5050 and 5500 gauss.

The level of oscillation could be adjusted so that the radiofrequency voltage developed across the coil varied between 0.1 and 1 V. This input would saturate most solids, and this method cannot therefore be used to plot the line shapes for solids at low temperatures. However, the oscillation is maintained at a very

steady level, even when the frequency is being changed. Alteration of frequency is simple with this circuit, which requires less adjustment than the frequency-sensitive bridge. Furthermore the spectrometer responds only to the absorption part of the resonance. These properties make this circuit invaluable for field measurement, and it was accordingly used, with a liquid sample, for calibration purposes.

(i) Calibration of Field Shift

The current through the field coils is measured by a millivoltmeter connected across a standard 0.2 ohm resistance box. A liquid line was observed on the screen of the C.R.O. using a field modulation of a few gauss. With no current flowing in the coils, the line was accurately centred. The frequency of resonance was measured, by lightly coupling a heterodyne frequency meter, Type EC 221, to the circuit, zero beat between the frequency of the oscillator and that of the meter being observed on the screen of the C.R.O. This procedure was repeated for several values of the current through the coils, for fields greater and less than the permanent magnet field  $H_0$ . The frequency shift per unit current

was then calculated, by inserting into the equation  $h\nu_0 = 2\mu H$  the values given by Bearden and Watt (1951):

$$h = 6.62563 \times 10^{-27} \text{ erg. sec.}$$

$$\mu_{\text{proton}} = 1.521026 \times 10^{-5} \text{ Bohr magnetons}$$

$$1 \text{ Bohr magneton} = 9.27100 \times 10^{-21} \text{ erg. gauss}^{-1}.$$

The method of least squares gave a value of 0.446 gauss/mV for the field shift.

#### (ii) Calibration of Modulation Coils

A similar procedure was used for the calibration of the modulation coils. When a sinusoidal voltage is applied to the coils and also to the X-sweep of the C.R.O. the trace gives a linear variation of field. For varying modulation amplitudes, the liquid line was observed at positions  $1/4$  and  $3/4$  along the X-sweep. The frequency difference was again converted into a difference in field, and the amplitude of the modulation found in terms of the 25 c/s current flowing in the coils.

#### (iii) Mapping of Magnet Field

It is advantageous to place the specimen in the most homogeneous



part of the magnet field. If the line is very narrow, it will be broadened to a value equal to the inhomogeneity of the field over the volume of the specimen. This would decrease the accuracy of the field calibration (i) and (ii), and is undesirable in the case of the very narrow lines sometimes observed with solid specimens.

The field strength was accordingly measured for various positions in the median plane, and the field "contours" drawn. The specimen was then positioned in the most homogeneous area. Over a sample of volume  $1 \text{ cm}^3$  the inhomogeneity was then about 0.25 gauss.

#### 3.4 Cooling Systems

Previous workers in this laboratory have used gas-flow cryostats to cool their specimens. This proved most satisfactory at temperatures down to  $70^\circ\text{K}$ , using liquid oxygen or nitrogen, pumped if necessary. It was, however, more efficient for relatively high temperatures: the lowest attainable temperature, was almost  $10^\circ$  above that of the pumped liquid nitrogen which evaporated rapidly when the cryostat was used in this temperature region. This gas-flow method would, therefore, be impracticable for use with liquid hydrogen.

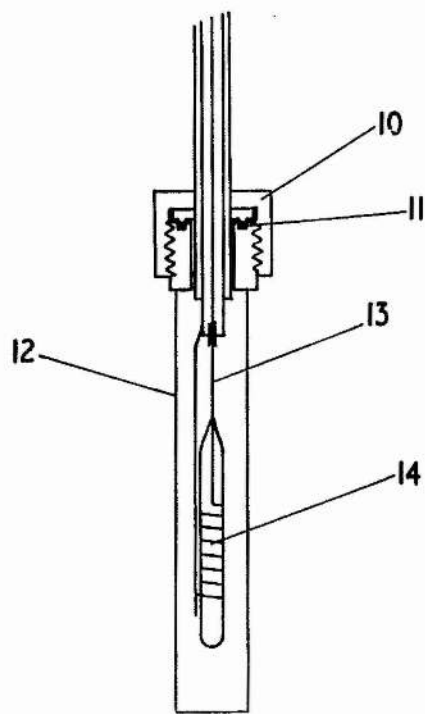
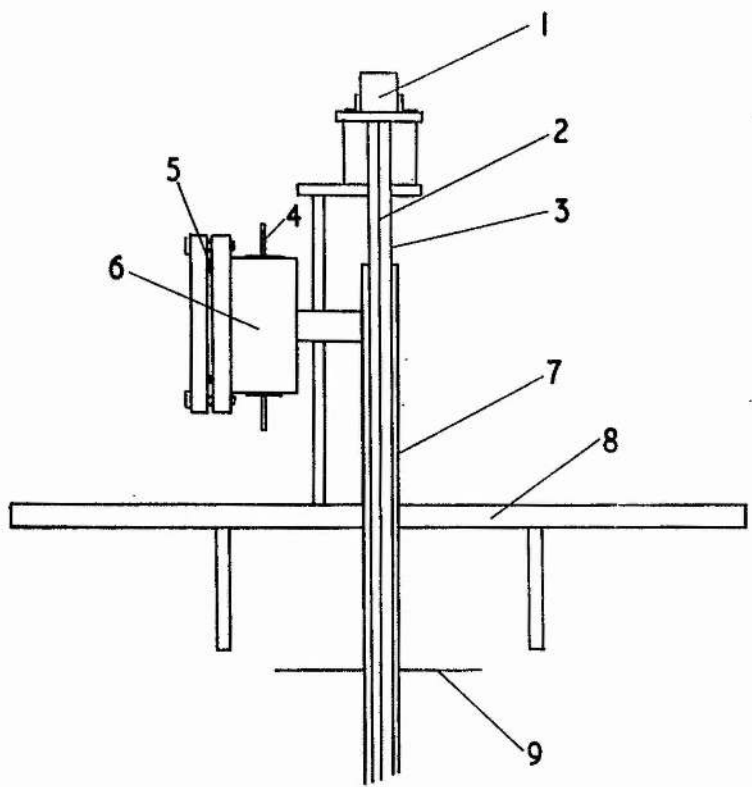


FIGURE 2

Moreover, liquid hydrogen would require the use of helium as the flow gas.

A cryostat suitable for use with liquid hydrogen was therefore designed and constructed. It is indicated schematically in figure 2 and is photographed in figure 3.

The specimen to be examined is sealed in a thin-walled Pyrex tube (14) of diameter 6 mm, supported in the coil. A typical coil consists of about 12 turns of 20 swg copper wire. Leads of 1 mm diameter copper-nickel alloy capillary tubing (13) support the coil, and connect it electrically to the main coaxial conductor. This consists of a 28 swg copper wire (2) running down the axis of a 6 mm thin-walled alloy tube (3), and supported at each end by Kovar seals. The copper wire at the top is connected to a coaxial socket (1), leading via a length of 75 ohm coaxial cable to the twin-T bridge. This coaxial conductor is surrounded by a 1 cm diameter thin-walled tube (7), which leads to a can (12) surrounding the coil and specimen tube. The can is rendered vacuum-tight by the indium ring-seal (11) and the coupling (10). Holes at the lower end of the 1 cm tube permit evacuation of the can through the

space between the concentric tubes. A wide tube at the top of the cryostat (not shown in figure 2) leads to a vacuum system consisting of a rotary pump, mercury diffusion pump and Pirani gauge. The whole assembly is fixed to a rigid brass plate (8), mounted above the magnet, and supported by four levelling screws to ensure accurate alignment of the specimen in the median plane of the magnet gap.

A heater is wound non-inductively on each end of the specimen tube, each heater consisting of 50 turns of 40 swg Eureka wire, and supplied by storage batteries. Between each heater and the coil is attached a copper-constantan thermocouple. The leads from the heaters and the thermocouples travel up the space between the concentric tubes, and are soldered to the Kovar seals (4) set in the rim of the connecting box (6). The connections are accessible via the front plate, and sealing is effected by the Gaco ring (5).

The Dewar to hold the liquid was "stepped", being narrow at the bottom to fit the magnet gap. It had a capacity of one litre. The dewar was filled by conventional methods: liquid hydrogen was transferred from the storage vessel under slight pressure, after the cryostat had been precooled with liquid nitrogen. A radiation

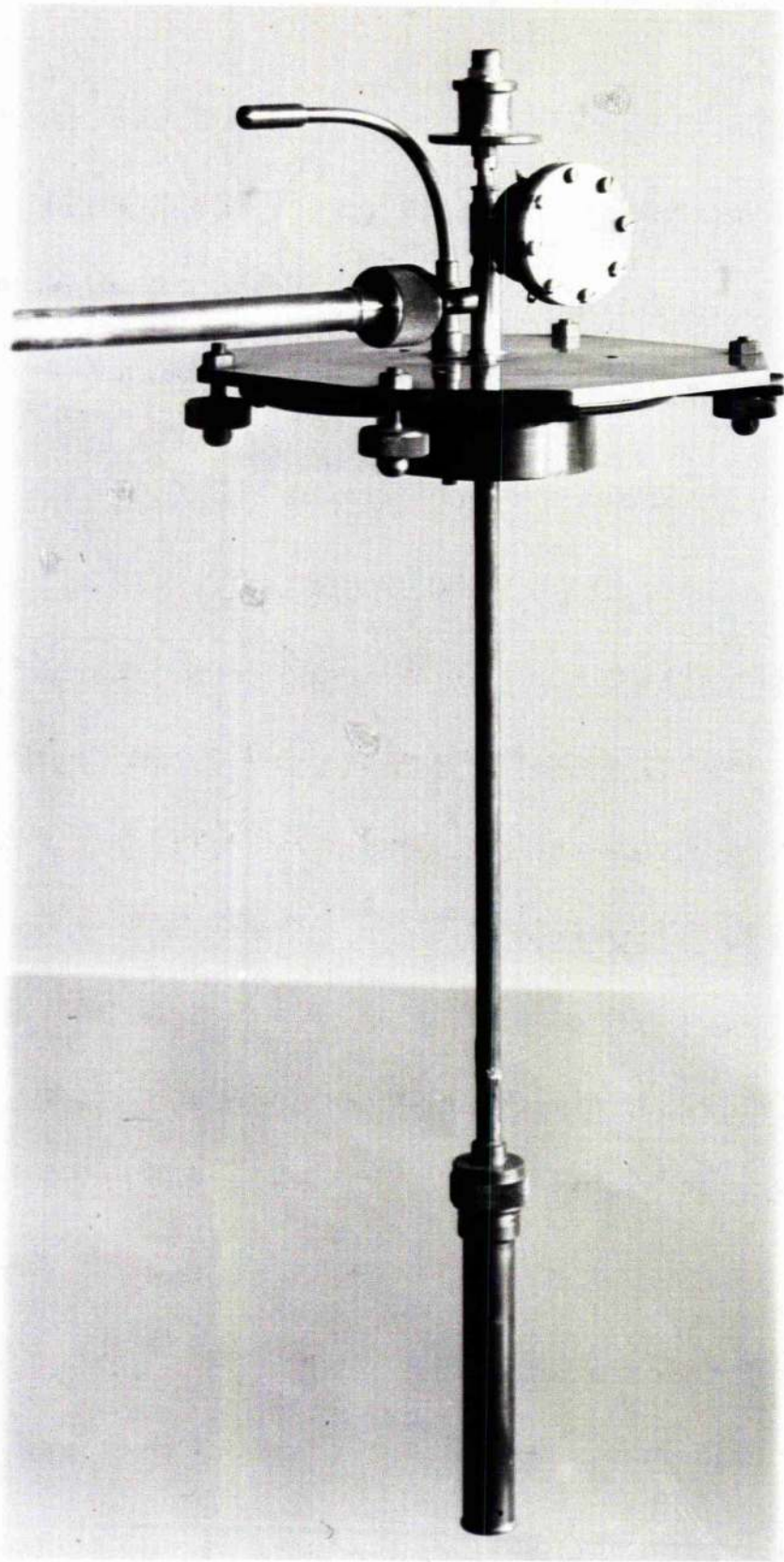


FIGURE 3



shield (9) of polished copper reduced the heat radiated down from the top plate of the cryostat to the liquid. Although only a single dewar was used the rate at which the liquid hydrogen boiled away - about 500 cc per hour - was quite satisfactory.

When the can is filled with hydrogen at a pressure less than atmospheric, there is thermal contact between the specimen and the liquid hydrogen. The specimen readily attains the temperature of the liquid hydrogen, the time to reach equilibrium being about 10 minutes. The heat input may be regulated by means of the heaters; the heat leaking from the specimen to the liquid depends on the pressure of the gas in the can. By altering these, varying temperatures may be attained, the separate heaters preventing temperature gradients across the sample. The equilibrium temperatures were very constant even over long periods of time. The same procedure applies to liquid nitrogen and oxygen except that in the case of liquid oxygen, dry air may be used as the thermal conductor.

Liquid hydrogen provides temperatures in the range 20°K to 45 °K, while liquid nitrogen and oxygen permit temperatures between 62°K and

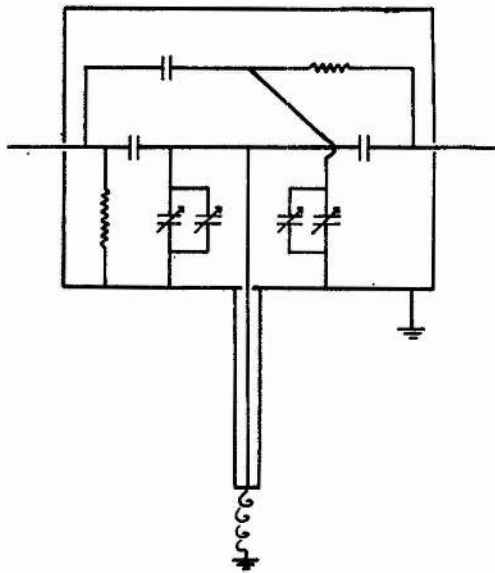
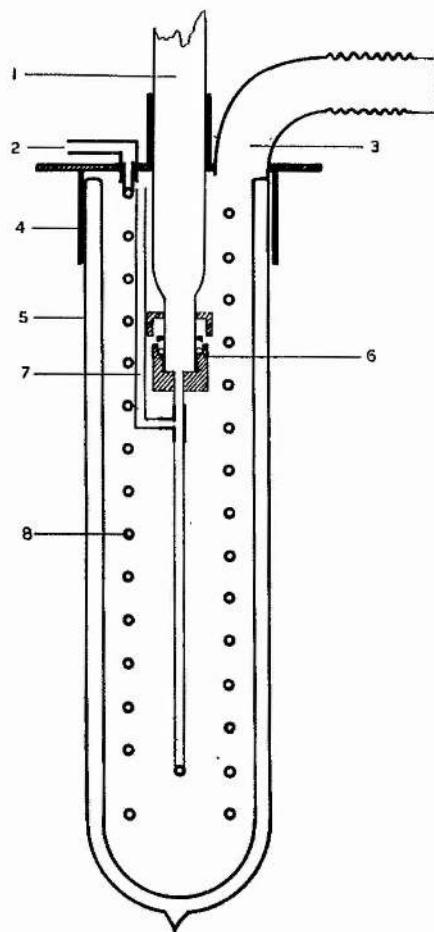


FIGURE 4



GAS CRYOSTAT.

FIGURE 5



140°K. Temperature measurements were all accurate to 1°, except possibly at the very lowest temperatures, where the thermoelectric voltage developed by the thermocouple varied less rapidly with temperature.

Figure 3 shows a photograph of the actual cryostat. Here we can see the broad pumping tube leading to the vacuum system, and also the narrow curved outlet tube from the Dewar, neither of which is shown in figure 2. The overall length of the assembly is 23 inches.

The investigation of cyclooctatetraene (section 4.5) however, required measurements at about 240°K, and for these the gas-flow method was used. This method has been fully described by Eades (1952). Dry gas is passed through a spiral (8, figure 5) immersed in liquid oxygen, and then up a long dewar tube (1) and over the specimen. The whole of the can was placed in the long dewar, hydrogen providing the thermal contact. Only one thermocouple, and no heaters were attached to the specimen tube in this case. By altering the rate of flow of the gas by a Rotameter flow gas, the temperature could be varied, and the required 240°K easily attained.

Great care was always taken to avoid supercooling of the specimen,



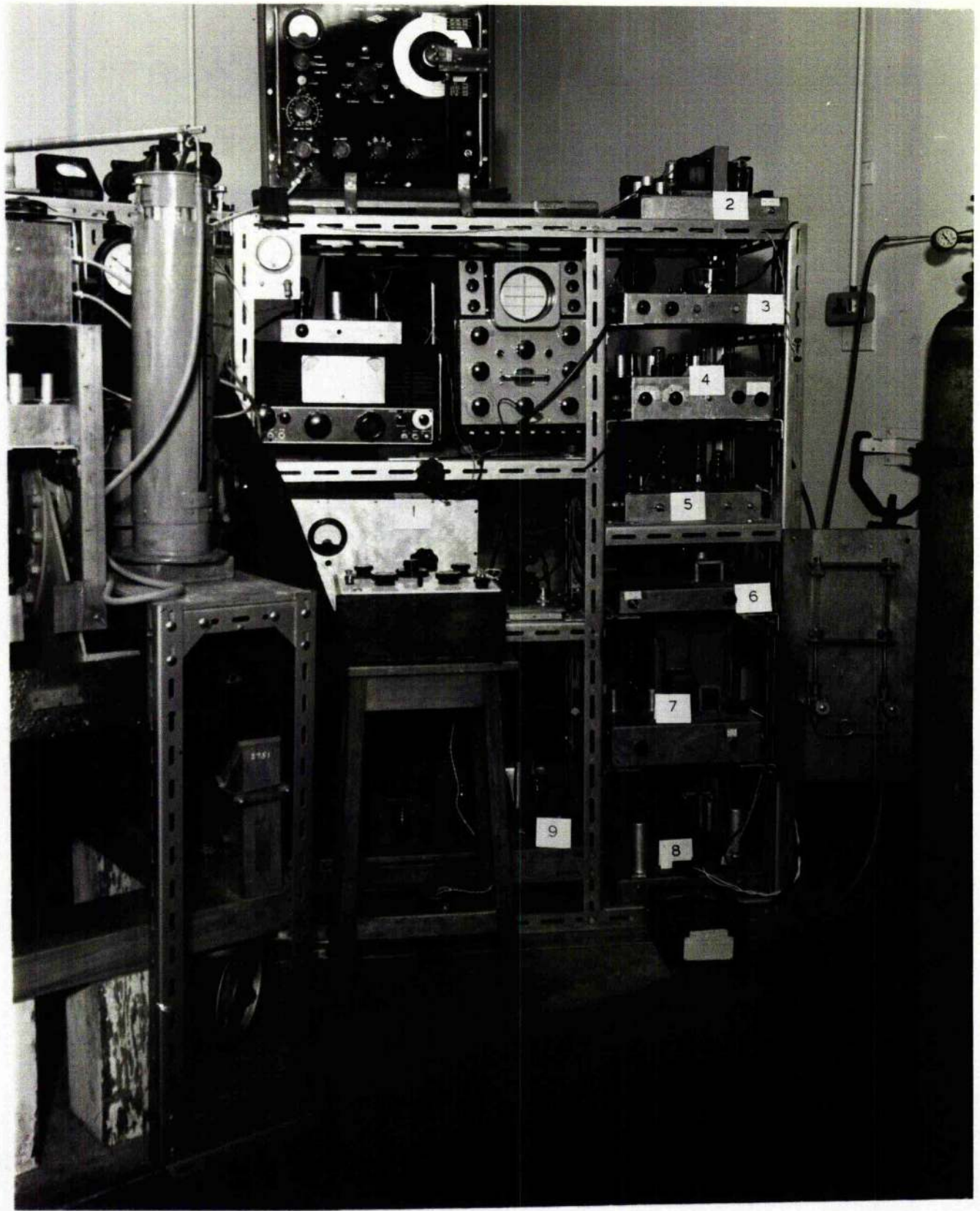


FIGURE 6



by cooling as much as possible, and then raising the temperature to the desired level. For instance the specimen of cyclooctatetraene was found to remain liquid even when placed in a freezing mixture at  $-16^{\circ}\text{C}$ , some  $10^{\circ}$  below the melting point.

In figure 6, is shown most of the electronic equipment. At the top is the Signal Generator, and immediately below this the Communications Receiver, signal-lever meter, and the Cossor Oscillograph, Type 1049. The other units are numbered and are:

- (1) Preamplifier, directly below the receiver.
- (2) Stabilised power supplies for receiver and preamplifier.
- (3) Phasing and transforming unit, supplying the X-sweep for the C.R.O.
- (4) Lock-in amplifier.
- (5) 25 c/s generator.
- (6) Power supplies for lock-in amplifier.
- (7) Power amplifier, feeding the modulation coils.
- (8) Power supplies for the power amplifier, and the 25 c/s generator.
- (9) Stabilised power supplies for the Signal Generator.

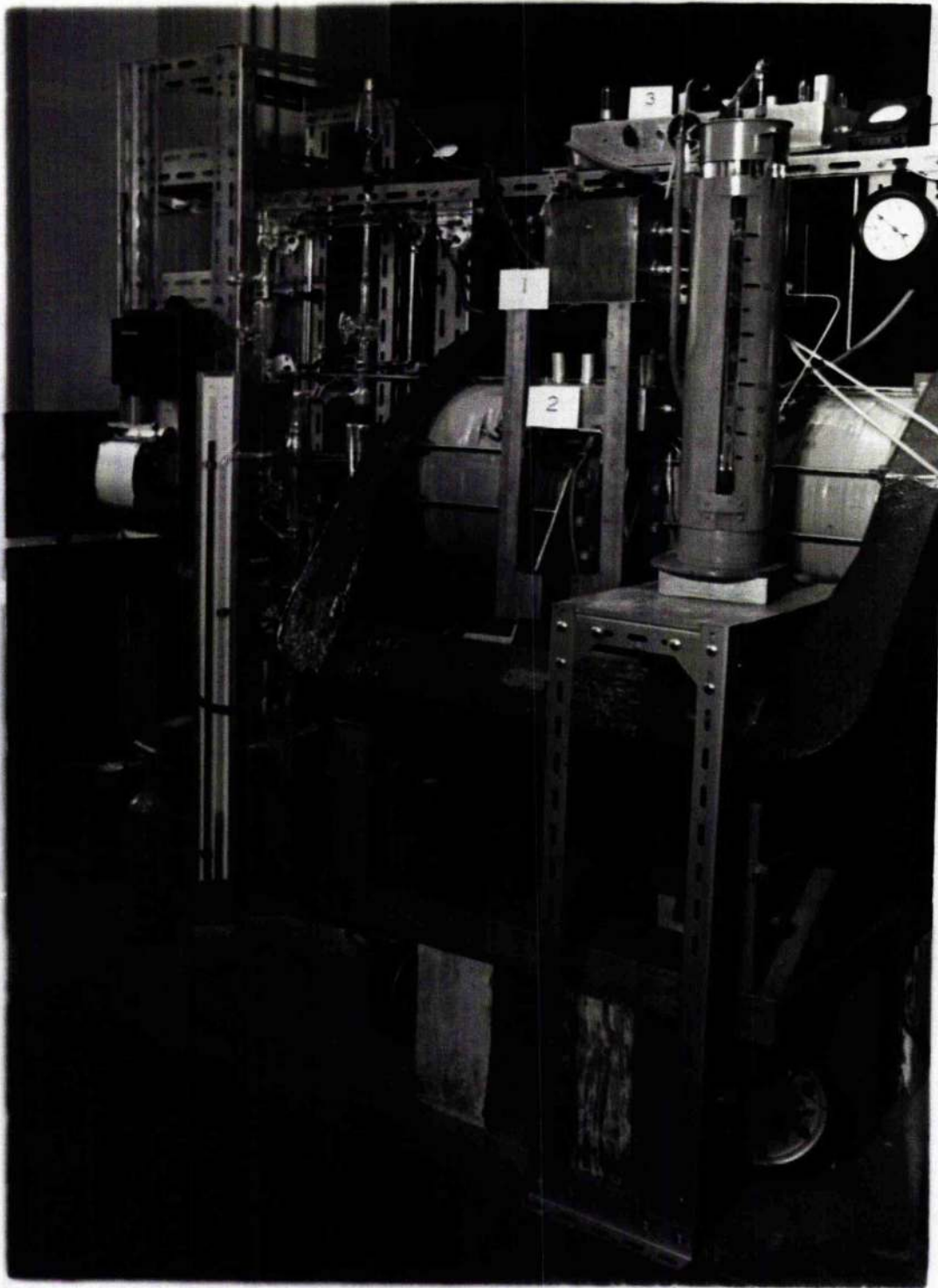


FIGURE 7



In front of the rack is the Doran thermocouple potentiometer. At the right are the cylinder of nitrogen gas and the flow-gauge, used for the gas-flow method of cooling.

At the extreme left is the liquid hydrogen storage vessel, which is shown again at the right of figure 7; in this photograph we can see:

- (1) Twin-T bridge.
- (2) "Cascode" amplifier.
- (3) Radiofrequency spectrometer.

The cryostat is situated directly behind the storage vessel, above the magnet gap. To the left of the permanent magnet is shown the vacuum system, and at the extreme left of the photograph is the Evershed and Vignoles recording microammeter, fitted with a 50 c/s synchronous motor drive.

4. EXPERIMENTAL RESULTS

#### 4.1 Choice of Subjects for Study

It is advantageous to use the proton as the nucleus at resonance: the high gyromagnetic ratio ensures a good signal strength (Bloembergen et al 1948) while with spin  $I = \frac{1}{2}$ , this nucleus has no electric quadrupole moment, present in nuclei with higher spin quantum numbers.

This thesis is concerned with nuclear magnetic resonance in hydrocarbons. These are ideal substances for investigation, as, apart from the proton, the only nucleus present in any appreciable quantity is carbon  $C^{12}$ , which has zero spin, making interpretation of the experimental results much easier. Hydrocarbon molecules contain a reasonably high proportion of hydrogen atoms, producing a good signal strength.

Structural investigations by X-rays normally indicate only the positions of the carbon atoms; the positions of the hydrogens have to be guessed. However, the local magnetic field, governing the width of the absorption spectrum, depends in general on the inter-proton distances and orientations in a rigid lattice; a measurement of the second moment may then verify the postulated positions of the protons in a molecule or crystal.



We have shown that the width of the absorption spectrum is reduced by molecular motion, even of a relatively low frequency. This is in contrast to the behaviour with X-rays, where molecular motion will be evident only when the mean rate of motion is of the order of the X-ray frequency ( $10^{18}$  c/s). This is also true for a neutron diffraction analysis, since the effective wavelength is similar to the X-ray wavelength ( $\sim 1 \text{ \AA}$ ).

Known physical properties such as specific heat, and infra-red and Raman spectra, are of interest when selecting subjects for study. For instance, a transition in the specific heat may indicate the possible sudden onset of molecular motion, which would give rise to a narrowing of the absorption spectrum. However, the reverse need not be true. Any molecular motion affects the absorption line only when the mean rate of reorientation is of the same order of magnitude as the line width. There is thus no great significance in the temperature at which the line width changes, and we should not in general expect a specific heat anomaly in this case. Thus, transitions in the line width may occur where there is no evidence of a specific heat anomaly.

The specimen examined must be of the highest purity. Any impurity present may affect the measured values of the spin-lattice relaxation time, and may even produce spurious line width changes; for instance, Rushworth (1952) found an apparent narrowing of the absorption line of anthracene, which was due entirely to the presence of an impurity, ethylene glycol.

The experiments reported in this thesis are concerned with problems of molecular motion and structure. Evidence for such motion in cyclopentane, n-pentane, n-hexane and n-octane, at temperatures down to 20°K, is discussed in sections 4.2 to 4.4. In section 4.5, it is shown how measurements of the absorption spectrum of cyclooctatetraene enable us to draw definite conclusions about the molecular structure of this compound.



4.2 CYCLOFENITENE (C<sub>11</sub>H<sub>13</sub>N)

CYCLOPENTENE ( $C_5H_8$ ).

4.2.1 Introduction

The specimen of cyclopentene examined was supplied by the Chemical Research Laboratory, Teddington, and had a mole per cent purity of  $99.97 \pm 0.02\%$ , as determined from freezing point measurements.

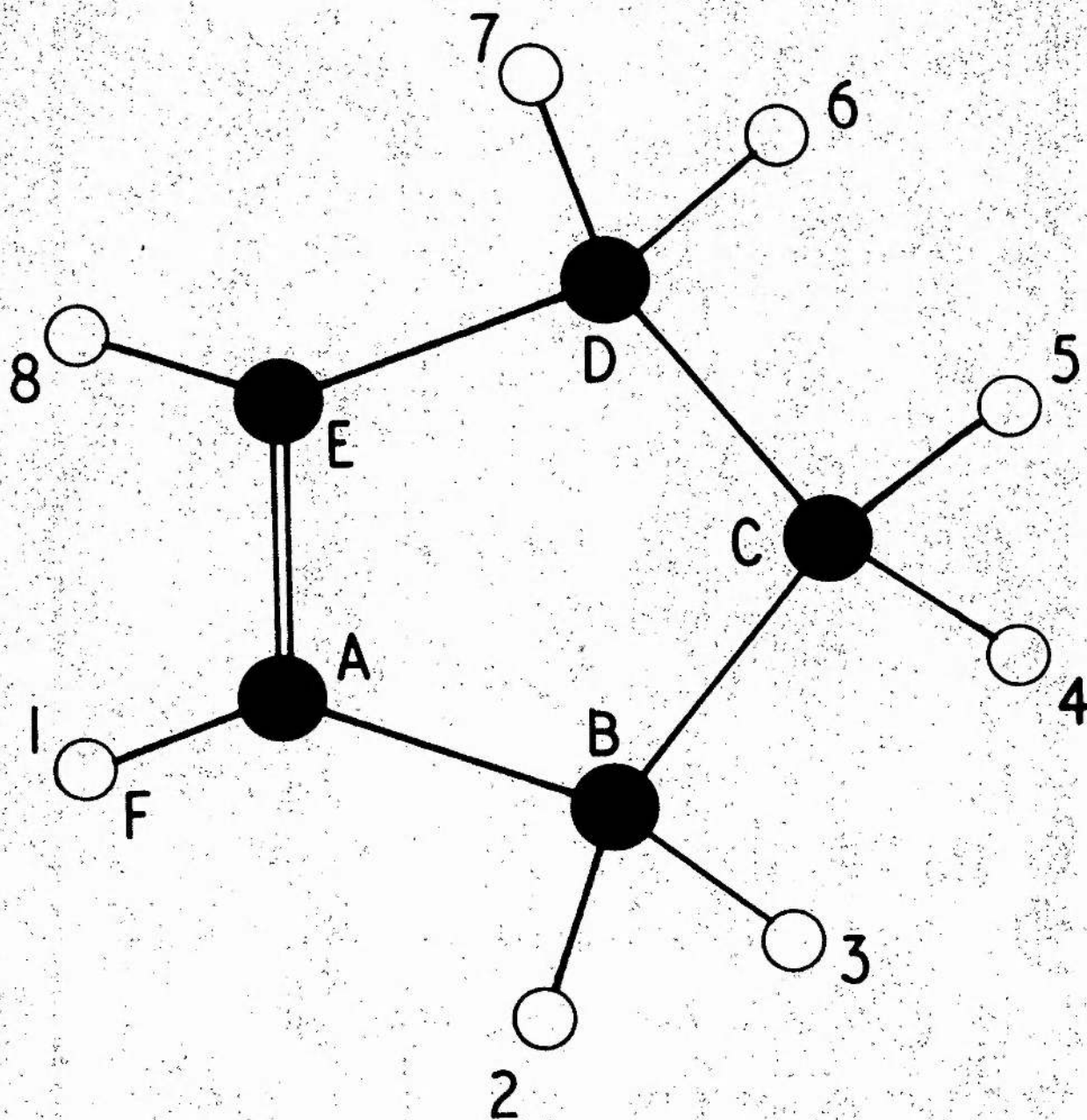
The sample was transferred from the standard ampoule in which it was supplied to a thin-walled, sealed Pyrex tube of diameter 6 mm specially made to fit the nuclear resonance coil.

4.2.2 Thermal Data

The specific heat from 20°K to room temperature, the transition temperature, and the heats of transition and fusion have been measured by H. M. Huffman, M. Eaton, and G. D. Oliver (1948). Their values for the heats of transition and fusion are:

	Temperature	Heat of transition or fusion, Cal/mole
Transition	87.07°K	114.6 $\pm$ 0.5
Fusion	158.13°K	803.9 $\pm$ 0.4

In addition these authors report a very slight anomalous behaviour



- Carbon atoms
- Hydrogen atoms

FIGURE 8

in the region of 54°K, the heat capacity changing to a higher value in a short temperature interval, which they attribute to the release of a frozen-in mode of motion.

#### 4.2.3 Molecular Structure

Beckett, Freeman and Pitzer (1948) have examined the molecular structure of cyclopentene. They assumed that carbon atoms ABDE (figure 8) were planar, since the torsional forces about the double bond are so much greater than those about the single bonds. If, however, carbon atom C also lay in this plane, the methylene groups would be opposed, giving bonds B-C and C-D their maximum torsional energy. Therefore, the total potential or strain energy was calculated as a function of the distance of carbon atom C from the plane of the other four, using known potential constants from analogous molecules. These authors then found that the potential was unchanged as carbon atom C was removed from the plane ABDE by any distance up to 0.3 Å.

Two molecular models are used in the analysis of the results: one is planar, the other has atom C removed from the plane of the other four by 0.3 Å. In both models the C-C bond is taken as 1.54

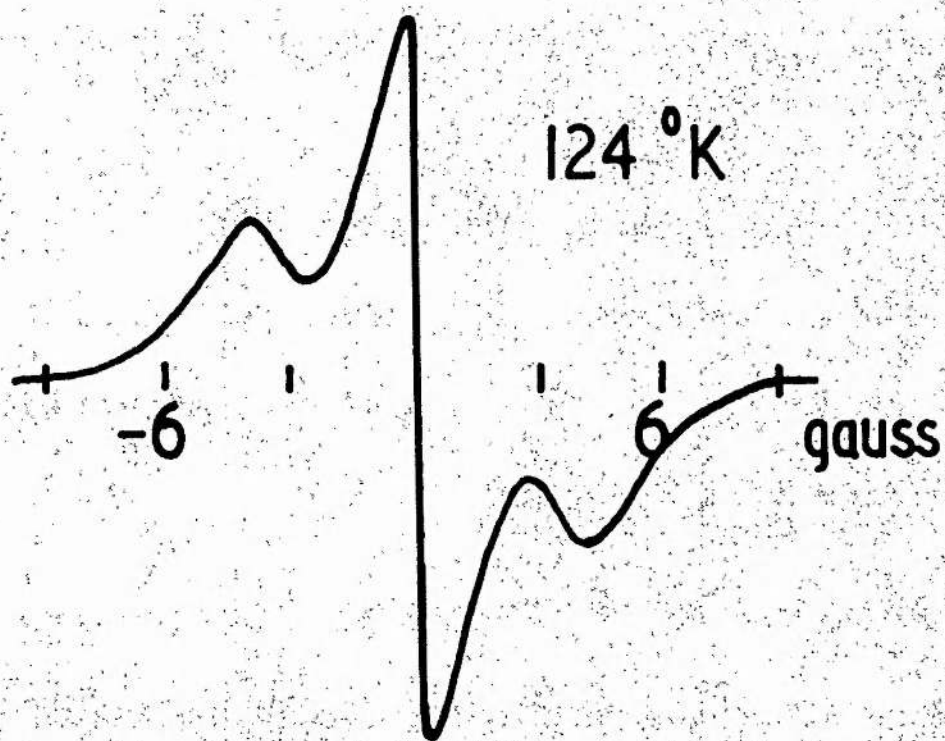
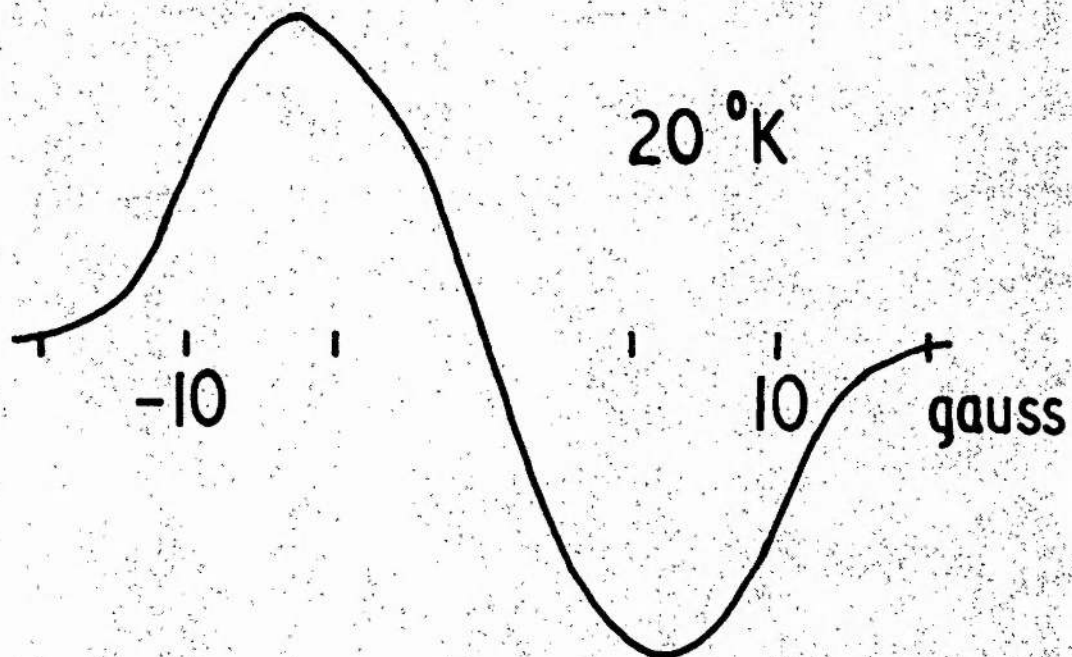


FIGURE 9



$\pm 0.01$  Å, and the C=C bond as  $1.34 \pm 0.01$  Å (Beckett et al 1948). The  $\text{>C-H}$  bond length is taken as  $1.10 \pm 0.01$  Å, on the basis of a determination of the bond lengths in ethane by Hansen and Dennison (1952), while the  $\text{>>C-H}$  bonds are taken as  $1.07 \pm 0.01$  Å (Herzberg 1945). The C-C-C angles at atoms B and D are assumed tetrahedral ( $109^\circ 28'$ ), as are the angles between the hydrogen bonds in each methylene group. Angle FAE is taken equal to BAE, and each proton pair is assumed to be inclined equally to the two C-C bonds. Using this geometry, the coordinates of each of the eight protons were calculated.

The crystal structure of cyclopentene has not been determined.

#### 4.2.4. The Absorption Spectrum

The first derivative of the absorption line shape was plotted at temperatures in the range of 20°K to the melting point, using the lock-in amplifier and recording meter.

The derivatives at 20°K and 120°K are shown in figure 9. It can be seen that the shape of the curve is quite different at these two temperatures: the fine structure first appears at about 96°K,

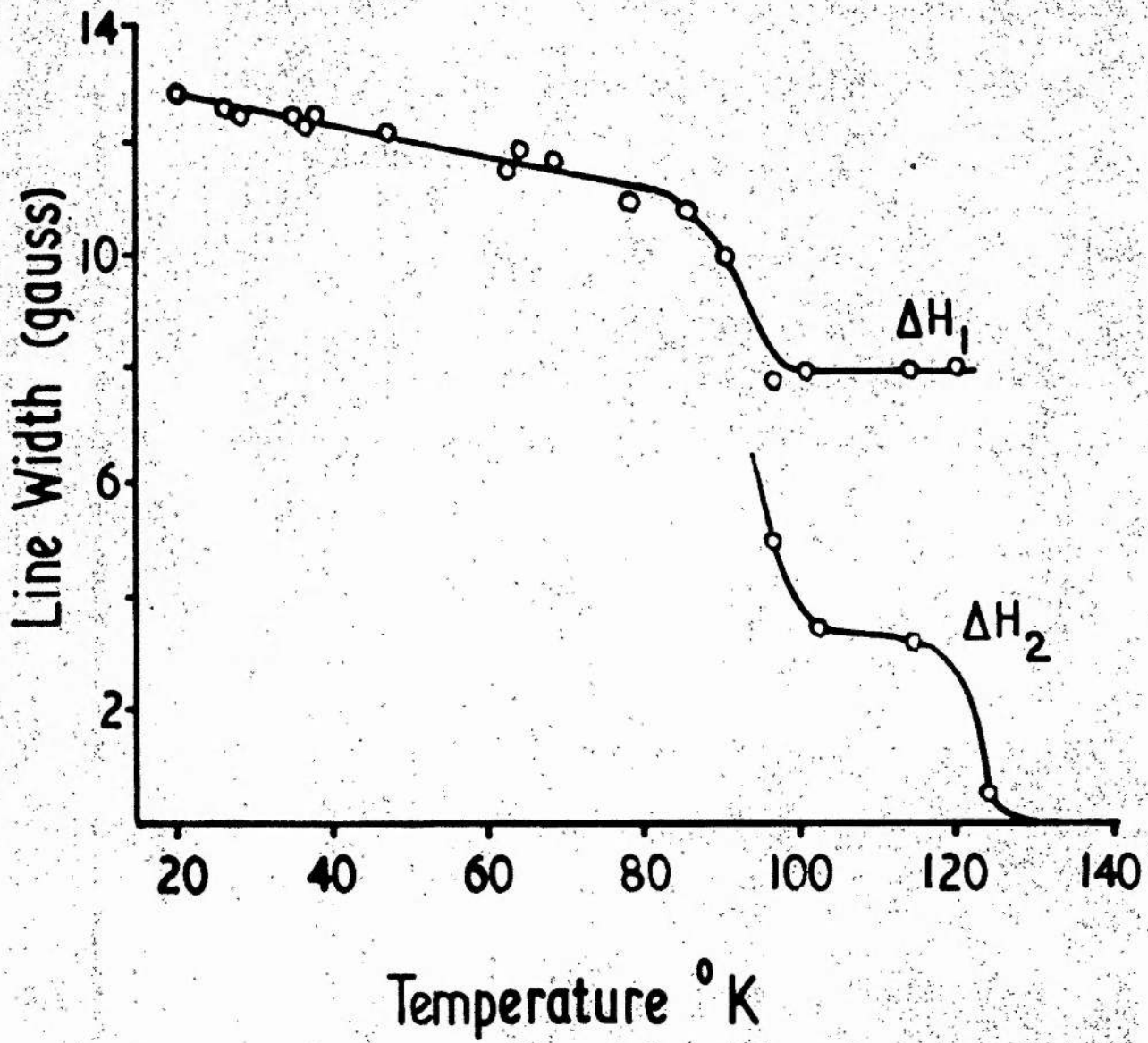


FIGURE 10



and will be explained later.

The line-width, defined as the interval in gauss between the points of maximum and minimum slope was measured, and is plotted as a function of temperature in figure 10. Because of the shape of the resonance line, two line-widths have been plotted at temperatures from 96°K upwards:  $\Delta H_1$  is the interval between two outer positions of maximum and minimum slope,  $\Delta H_2$  is the interval between the two inner positions.

It has been shown (equation 6) that the second moment is given

by:

$$\langle (\Delta H)^2 \rangle_{av} = \frac{1}{3} \cdot \frac{\int h^3 \frac{df(h)}{dh} dh}{\int h \frac{df(h)}{dh} dh}$$

The quantity  $df(h)/dh = F(h)$  is precisely the reading indicated on the output meter, in arbitrary units. The integrals are evaluated directly using the trapezium rule,

$$\text{i.e. Second Moment} = \frac{1}{3} \frac{\sum h^3 F(h)}{\sum h F(h)} \quad (14)$$

This equation is used throughout to calculate the experimental second moments.

The experimental values of the second moment must be corrected



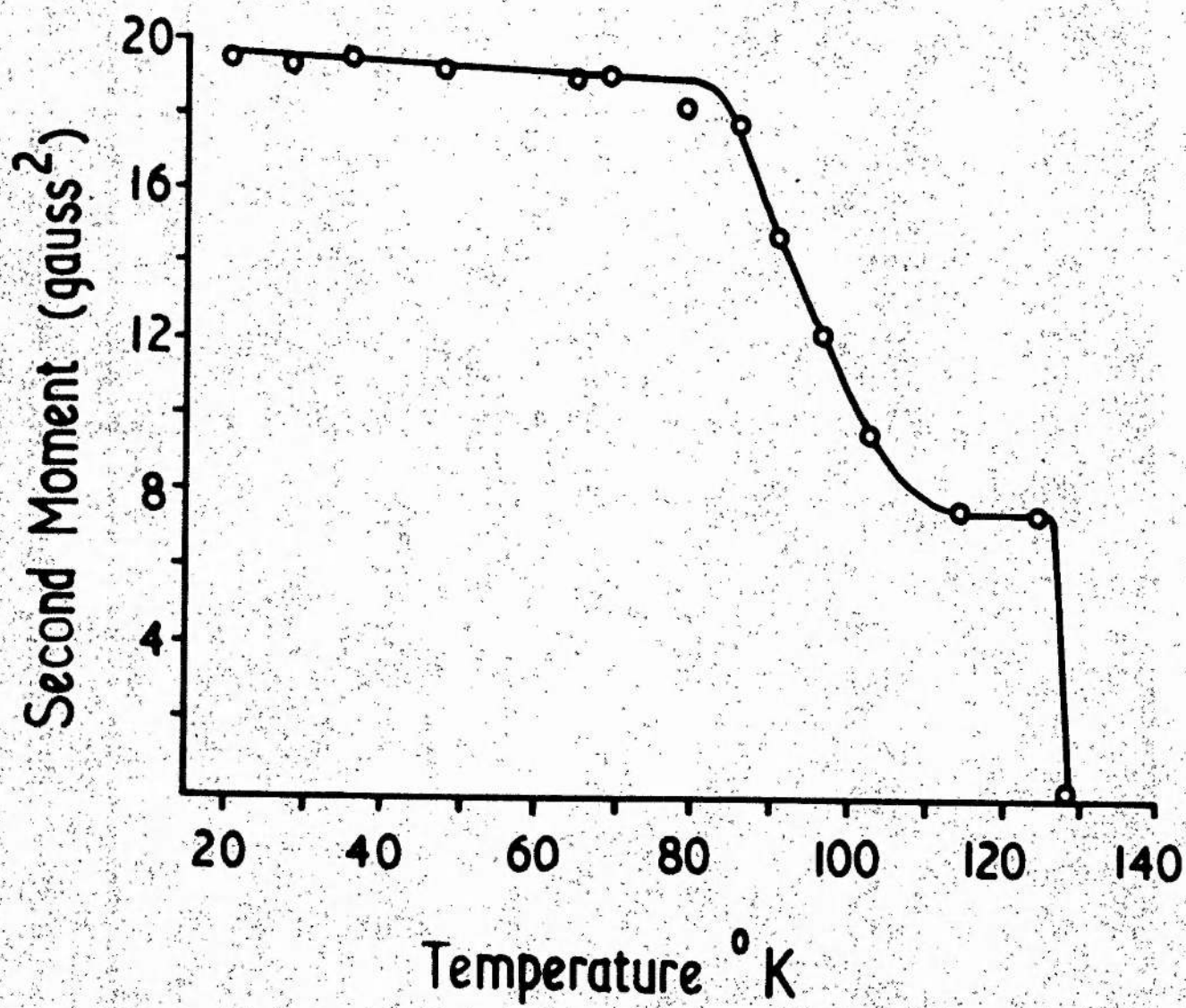


FIGURE 11.

for the broadening of the absorption line by the finite modulation of the magnetic field. Andrew (1955) has shown that, if  $S'_2$  is the measured value of the second moment, found from equation 14, then the true second moment  $S_2$  is given by

$$S'_2 = S_2 + \frac{1}{4} h_m^2 \quad (15)$$

where  $h_m$  is the amplitude of the field modulation.

The second moment is shown as a function of temperature in figure 11. It can be seen that below 85°K the line width and second moment values are steady, suggesting that the lattice is effectively rigid at these temperatures. Both quantities decrease slightly as the temperature is raised, due mainly to thermal expansion of the lattice. The mean experimental value of the second moment at 20°K is  $19.6 \pm 0.25$  gauss<sup>2</sup>. Experimental errors quoted throughout this thesis are in fact the standard deviations of the experimental results. A theoretical value for the second moment has been calculated, using both the molecular models described in section 4.2.3. In such calculations it is convenient to divide the second moment into two parts: an intramolecular contribution, describing the

interactions between protons in the same molecule, and an intermolecular contribution due to interactions between molecules. The plane model then provides an intramolecular second moment of  $12.9 \text{ gauss}^2$ , while the non-planar molecule gives a value of  $13.0 \text{ gauss}^2$ . In each case, about 60% of this total is provided by the interactions between the pair of protons in each methylene group. The intermolecular contribution to the second moment cannot be calculated exactly, as the crystal structure is unknown. However, the experimental value for the intermolecular second moment,  $6.6 \pm 0.35 \text{ gauss}^2$ , may be compared with values found for similar hydrocarbon molecules with known crystal structures.

The most similar molecule investigated, having a known crystal structure, is cyclohexane (Andrew and Eades 1953a); the theoretical value for the intermolecular second moment of this substance is  $10 \text{ gauss}^2$ . Thus, the ratio of the experimental value for cyclopentene to the theoretical value for cyclohexane is  $6.6/10$ , very nearly the ratio of the number of protons in each molecule. While this relationship is, in a sense, fortuitous, it does show that the experimental value is of a reasonable magnitude for a rigid lattice,

and suggests that the two molecules are packed similarly in their respective lattices. Other calculated values for the intermolecular second moment are generally in the range 4 to 10 gauss<sup>2</sup> - e.g. 6.52 gauss<sup>2</sup> for benzene (Andrews and Eades 1953b), 4.88 gauss<sup>2</sup> for anthracene (Rushworth 1952) - supporting the assumption of a lattice rigid at 20°K.

At about 85°K, corresponding to the specific heat transition, the absorption line starts to narrow, and both second moment and line width values are reduced. The second moment drops to a value of  $7.6 \pm 0.2$  gauss<sup>2</sup> at 110°K, while the absorption line begins to show the fine structure previously mentioned. There is no observable change in the line width or second moment at 54°K, the temperature of the slight anomalous effect in the specific heat reported by Huffman et al (1948): if there were the release of a frozen-in mode of motion at this temperature, as these authors suggest, the absorption line would probably show changes in width and shape, provided, of course, that the motion was sufficiently rapid.

The observed line narrowing between 85°K and 110°K may be



explained on the basis of molecular motion. The motion most likely to occur is rotation about an axis perpendicular to the plane of the four carbon atoms A, B, D, E. During this motion, protons from adjacent molecules approach one another less closely than in the case of rotation about other axes. This axis is not a multiple symmetry axis, and so classical rotation is the only motion possible.

The effect of this motion on both molecular models was investigated, using a modified form of the Van Vleck formula (Gutowsky and Pake 1950). For classical rotation, or  $n$ -fold tunnelling ( $n \geq 3$ ) about a symmetry axis of the molecule, each term in the Van Vleck formula is multiplied by a reduction factor

$$\rho = \frac{1}{4} (3 \cos^2 \gamma_{jk} - 1)^2 \quad (16)$$

$\gamma_{jk}$  being the angle between the internuclear vector joining nuclei  $j$  and  $k$ , and the axis of rotation. Multiplication by this factor has the effect of averaging the term  $(3 \cos^2 \theta_{jk} - 1)^2$  over the motion.  $\rho$  decreases from unity ( $\gamma_{jk} = 0$ ) to zero ( $\gamma_{jk} = 54^\circ 44'$ ) and increases again to  $\frac{1}{4}$  ( $\gamma_{jk} = 90^\circ$ ).

In the planar case the reduction in the second moment is slight, as the interproton vector in each methylene group is exactly parallel

to the axis of rotation; the interactions between the proton pairs in the methylene groups dominate the rigid lattice value, and so there is only a small reduction. The reduced value is  $9.4 \text{ gauss}^2$ ,  $8.4 \text{ gauss}^2$  of which is contributed by the  $\text{CH}_2$  groups. In the non-planar case, however, the reduction is greater: the intramolecular contribution to the second moment is reduced to  $6.7 \text{ gauss}^2$ .

For the intermolecular contribution to the second moment, comparison must again be made with similar molecules with known crystal structure. In the case of cyclohexane, Andrew and Eades (1953a) show that motion about the corresponding axis reduces the intermolecular second moment by a factor 0.24. Because of the possibility of similar packing mentioned previously, we might expect the intermolecular contribution in the case of cyclopentane to be reduced by approximately the same factor; this gives a value of  $1.6 \text{ gauss}^2$ , with a large uncertainty, say  $\pm 0.5 \text{ gauss}^2$ .

The total second moment for the non-planar molecule is thus  $8.3 \pm 0.5 \text{ gauss}^2$ , in satisfactory agreement with experimental value of  $7.6 \pm 0.2 \text{ gauss}^2$ , considering the lack of knowledge concerning the crystal structure. Because of the lack of symmetry of the

molecule, there might be a slight rocking motion, associated with the rotation, which would further reduce the second moment by a slight amount. Motion about the corresponding axis in the planar case cannot explain the second moment reduction, as the reduced intramolecular contribution alone is greater than the experimental value for the total second moment.

Reorientation about the two-fold axis passing through the midpoint of the double bond, and carbon atom C, is possible, at least in the plane molecule, and must be considered. For rotation about a diad axis the reduction factor to be applied to the Van Vleck equation is

$$\rho' = (1 - 3 \sin^2 \gamma_{jk} \cos^2 \gamma_{jk})$$

$\gamma_{jk}$  again being the angle between the interproton vector and the axis of rotation (Eades 1952). This factor falls from unity ( $\gamma_{jk} = 0$ ) to 0.25 ( $\gamma_{jk} = 45^\circ$ ), and then rises again to unity ( $\gamma_{jk} = 90^\circ$ ). This motion produces a sufficient reduction with neither model, as the principal interproton vectors are almost perpendicular to the axis of rotation.

Thus, it appears most likely that the cyclopentene molecule is



not plane, but has one atom removed from the plane of the other four by approximately 0.3 Å, and at about 85°K the whole molecule starts to rotate about an axis perpendicular to the plane of the four atoms.

The absorption line undergoes a further rapid narrowing between 124°K and 128°K, so that at this temperature, 10° below the melting point the second moment and line width both have the values found for the liquid line, determined by the field inhomogeneity over the volume of the specimen.

If free rotation of the molecules were taking place, the intramolecular second moment would be reduced to zero: the effect on the intermolecular second moment would not be so drastic. An exact value cannot be calculated, but we should expect the intermolecular contribution to be reduced to about 1 gauss<sup>2</sup> (Andrew and Eades, 1953a; Rushworth 1954). This motion is, therefore, insufficient to explain the experimental data.

We have thus used up all three rotational degrees of freedom, and are left with only the translational degrees of freedom. Self-

diffusion of the molecules through the lattice has been reported in several hydrocarbons, (Andrew 1954): this reduces the time-averaged intermolecular field to zero, and could produce the very narrow line observed. Any molecular motion affects the absorption line only if the mean frequency of the motion is of the order of the line width expressed as a frequency ( $10^{14}$  c/s). The molecules, therefore, must make approximately  $10^{14}$  random jumps per second between adjacent vacancies at 124°K, when this process is beginning to affect the line width.

We must now explain the fine structure of the absorption line. The protons in the cyclopentene molecule are divided into two classes: those lying in pairs (protons 2 - 7, figure 8) and those relatively distant from their nearest neighbours (protons 1 and 8). The absorption line should therefore be a superposition of the curves for a single proton and for a proton pair. The proton pair in a polycrystalline solid give an absorption curve with two peaks separated by  $3\mu/d^3$ , where  $d$  is the distance between the two protons. However, for the rigid lattice, the overall interactions are too large and obscure the curve obtained from the proton pair. When the molecule

starts to rotate, this is no longer the case. All the interactions are reduced, but the interactions between the proton pairs in the methylene groups are reduced less, as the interproton vector in each case is almost parallel to the axis of rotation. Of the reduced intramolecular contribution of 6.7 gauss, 5.9 gauss<sup>2</sup> is provided by the  $\text{-CH}_2$  groups. Under these circumstances we should expect the absorption line to be a combination of the curves for a pair and a single proton. This is the form of the observed line (figure 9).

The interproton separation is 1.796 Å, using the bond lengths and angles assumed in the calculation of the second moment: this corresponds to a separation of 7.3 gauss between the two peaks in the proton pair absorption curve. While it is impossible to measure the exact separation on the combined absorption curve, it can be seen that it will be less than the value of 8 gauss found for  $\Delta H_1$ ; this agreement supports this explanation of the fine structure.

The results obtained for cyclopentene may be summarised as follows:

- (1) The lattice is effectively rigid between 20°K and 85°K.

There is no evidence of the onset of molecular motion at 54°K, corresponding to the specific heat anomaly reported by Huffman et al (1948), and attributed by them to the release of a frozen-in mode of motion.

(ii) The absorption line starts to narrow at 85°K, approximately the transition temperature found by Huffman et al. This resonance line width change can be correlated with rotation of the molecule provided a non-planar molecular model is taken.

(iii) At approximately 125°K, self-diffusion of the molecules through the lattice occurs, reducing the line width rapidly, so that at 128°K, 10° below the melting point, the line-width is less than the field inhomogeneity over the volume of the specimen.

4.3 n-PENTANE ( $C_5H_{12}$ ) and n-HEXANE ( $C_6H_{14}$ )

n-PENTANE ( $C_5H_{12}$ ) and n-HEXANE ( $C_6H_{14}$ )

4.5 The absorption spectra and the spin-lattice relaxation times have been measured from 70°K to the melting points by Rushworth (1954). The second moments of the absorption lines were found to be less than the calculated values for rigid lattices over the entire temperature range. The values quoted for 120°K are:

	Rigid lattice Second Moment	Experimental Second Moment
n-Pentane	$31.0 \pm 2.0 \text{ gauss}^2$	$16.7 \pm 0.7 \text{ gauss}^2$
n-Hexane	$30.6 \pm 2.0 \text{ gauss}^2$	$18.8 \pm 0.7 \text{ gauss}^2$

Rushworth showed that the measured values for the second moment were in agreement with theoretical values for molecules in which the methyl groups were rotating about the end C-C axes.

Andrew (1950) has suggested the possibility of some form of molecular motion in the higher homologues, octadecane ( $nC_{18}H_{38}$ ), octacosane ( $nC_{28}H_{58}$ ) and dicetyl ( $nC_{32}H_{66}$ ) at 95°K.

The second moments and line-widths were measured at 20°K.

The values obtained were:



	Second Moment ( $G^2$ )	Line Width (G)
n-Pentane	$21.2 \pm 0.6$	13.8
n-Hexane	$21.4 \pm 0.8$	12.8

There is a slight increase in the second moments due to lattice contraction. However, the total experimental second moments are approximately equal to the intramolecular contributions for rigid lattices, showing that reorientation of the methyl groups is still occurring.

The same specimens were used as by Rushworth. They were supplied by the Chemical Research Laboratory, and had quoted purities of  $99.98 \pm 0.06$  and  $99.85 \pm 0.05$  mole per cent for n-pentane and n-hexane respectively.

4.4 n-OCTANE (C<sub>8</sub>H<sub>18</sub>)

n-OCTANE ( $C_8H_{18}$ )

4.4.1 Introduction

A study of the molecules n-pentane and n-hexane (section 4.3) has shown that considerable molecular reorientation is occurring even at temperatures as low as 20°K. It was decided, therefore, that an investigation of the absorption spectrum of the higher homologue n-octane, might be of interest; the greater size and mass of this molecule might cause the lattice to become rigid at some convenient temperature within the range of the cryostat. The melting and boiling points of n-octane are higher than those of n-pentane and n-hexane, and so we can operate over a greater temperature range in which the specimen is solid.

The specimen was obtained from the Chemical Research Laboratory, Teddington. The quoted purity was  $99.63 \pm 0.18$  mole per cent, as determined from measurements of the freezing point.

As for the other samples examined, the n-octane was transferred to a 6 mm thin-walled Pyrex tube fitting the resonance coil.

#### 4.4.2 Thermal Data

The specific heat of n-octane has been measured from 90°K to the melting point by Huffman, Parks and Barnore (1931). No specific heat transition was found in this temperature range.

The following data is quoted by Timmermans (1950):

	Temperature	Heat of Melting
Freezing Point	= 56.8°C	43.21 cal/g
Boiling point	125°C	

#### 4.4.3 Molecular and Crystal Structure

The molecular and crystal structure of the series of n-paraffins  $C_nH_{2n+2}$  has been investigated by Müller (1928, 1930, 1932) using X-ray diffraction techniques. The structure of  $C_{29}H_{60}$  he found exactly, using a single crystal. The molecule consists of plane zig-zag chains of carbon atoms, with tetrahedral angles ( $109^\circ 28'$ ) between the C-C bonds. The length of the C-C bond is 1.54 Å. The unit cell of the crystal lattice is orthorhombic, with dimensions  $a = 7.45$  Å,  $b = 4.97$  Å,  $c = 77.2$  Å. The carbon chains are then arranged parallel to the c-axis of the

unit cell.

Müller has also investigated other members of the series  $C_n H_{2n+2}$  for values of  $n$  between 5 and 30, using powder photographs, and showed the structures to be similar to that of  $C_{29} H_{60}$ . The  $a$  and  $b$  dimensions of the unit cells remain constant and equal to the values quoted for  $C_{29} H_{60}$ . The  $c$  dimension changes, however, increasing by about 2.5 Å for each additional  $CH_2$  group.

In the work reported here, tetrahedral angles between carbon bonds of length 1.54 Å are assumed; the C-H bond length is taken as 1.10 Å, on the basis of the determination of the bond lengths and angles in ethane, the lowest member of the series, by Hansen and Dennison (1952).

#### 4.4.4. Absorption Spectrum

The first derivative of the absorption line shape was plotted at 20°K, 90°K and 120°K, using the lock-in amplifier and recording meter.

The line width, defined as usual as the interval in gauss



between positions of maximum and minimum slope was measured.

Values found were:

	Line width (G)
20°K	14.5
90°K	13.9
120°K	12.3

The second moments were calculated using equation (14), and were corrected for spurious broadening due to the finite field modulation, using equation (15).

	Second moment (G <sup>2</sup> )
20°K	21.4 ± 1.0
90°K	20.5 ± 0.4
120°K	18.8 ± 0.4

The quoted errors are again the standard deviation about the mean of the results.

Thus, in the temperature range 20°K to 120°K there is no appreciable change in either line width or second moment. Both quantities show a slight increase as the temperature is lowered, due to thermal contraction of the lattice.

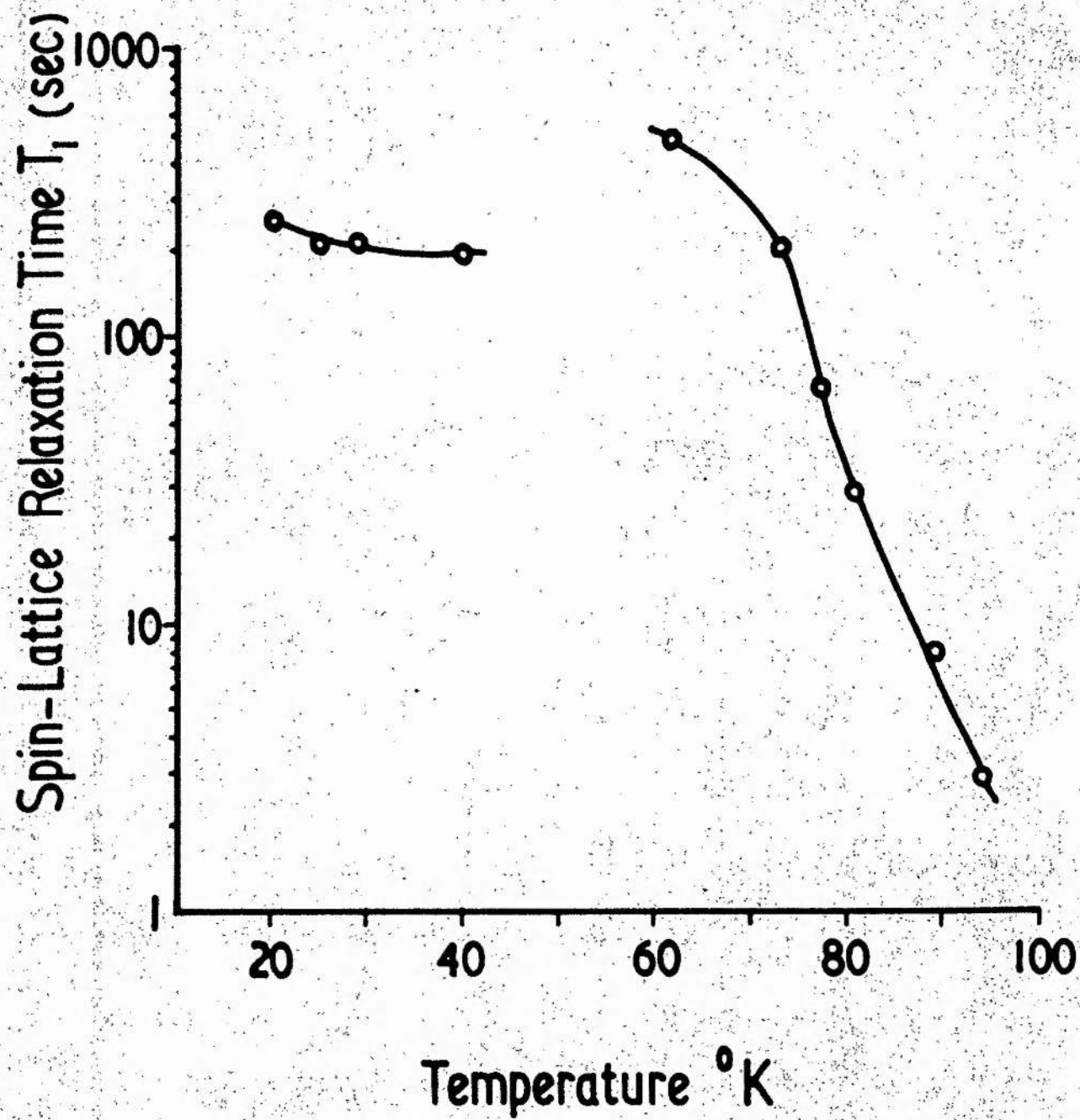


FIGURE 12

Fine structure is evident in the absorption line shape at all three temperatures. The derivative curve shows a slight secondary maximum and minimum corresponding to a small central peak on the actual line shape. This structure is reasonably similar to that observed by Andrew (1950) for  $C_{18}H_{38}$ ,  $C_{28}H_{58}$  and  $C_{32}H_{66}$ .

#### 4.4.5 Spin-Lattice Relaxation Time

The spin-lattice relaxation time  $T_1$  was measured at temperatures between 20°K and 100°K. The experimental results obtained are shown as a function of temperature in Figure 12.

Two methods were used to measure this relaxation time. For the longer values of  $T_1$  the direct method was employed. The biasing field is adjusted so that the output meter reads either the maximum or minimum value of the derivative of the absorption line, using a suitable modulation amplitude. The radiofrequency field  $H_1$  must be small enough to avoid saturation (equation 13). The radiofrequency input level is then increased by 30 or 40 db;  $\gamma^2 H_1^2 T_1 T_2$  increases and the specimen is saturated. When the

input level is suddenly restored to its original value, the observed signal recovers exponentially, according to the relation  $(1 - e^{-t/T_1})$  and so the spin-lattice relaxation time can be measured directly. This relation applies strictly only to recovery in the absence of a radiofrequency field. It is important, therefore, that the lower input level is low enough to avoid appreciable saturation. In practice the recovery of the signal was observed on the recording meter, giving a permanent record of the exponential rise. It was found advantageous to avoid overloading of the receiver input when the radiofrequency input level was increased, and so the preamplifier H.T. was switched off during this period.

This direct method can be used for values of  $T_1$  from 30 seconds upwards. For relaxation times less than this, the progressive saturation method was used. It has already been shown that the saturation factor  $Z_0$  is a function of  $T_1$ :

$$\frac{n}{n_0} = \frac{1}{1 + \gamma^2 H_1^2 T_1 T_2} = Z_0 \quad (\text{equation 13})$$

$T_1$  can therefore be determined by a study of the saturation process itself. The readings of the output meter, assumed proportional to

$n_2$  are plotted against the radiofrequency input level. As the input level is increased, so is  $H_1$ , and the signal strength accordingly falls, assuming half the maximum value when

$\gamma^2 H_1^2 T_1 T_2 = 1$ . If such curves are plotted at two temperatures  $T_A$  and  $T_B$ , then at the half-value points

$$(\gamma^2 H_1^2 T_1 T_2)_A = (\gamma^2 H_1^2 T_1 T_2)_B$$

Thus,

$$\frac{(T_1)_B}{(T_1)_A} = \frac{(H_1^2 T_2)_A}{(H_1^2 T_2)_B}$$

$(T_2)_A / (T_2)_B$  is the ratio of line widths  $\Delta H_B / \Delta H_A$ , assuming the curves are geometrically similar at the two temperatures, and

$(H_1^2)_A / (H_1^2)_B = V_A^2 / V_B^2$ , where  $V_A, V_B$  are the radiofrequency inputs corresponding to  $(H_1)_A, (H_1)_B$ . Thus we obtain,

$$\frac{(T_1)_B}{(T_1)_A} = \left(\frac{V_A}{V_B}\right)^2 \frac{\Delta H_B}{\Delta H_A}$$

The progressive saturation method therefore, gives relative values of the spin-lattice relaxation time. These can be converted to absolute values provided a direct measurement is possible at one temperature, in this case at 80°K, where  $T_1$  equalled 30 seconds.



However, this method assumes that the line shape remains constant even when the specimen is being saturated. This will not in general be exactly correct; equation (12) shows that the amount of saturation varies with the position in the absorption line, and so we should expect the line shape to alter somewhat.

The progressive saturation method applies only when  $\omega_m T_1 \ll 1$  or  $\omega_m T_1 \gg 1$  where  $\omega_m/2\pi$  is the modulation frequency. In all the values of  $T_1$  shown in figure 12, the condition  $\omega_m T_1 \gg 1$  does in fact apply.

Relaxation time measurements are subject to considerable inaccuracies. When the direct method is used the scatter of the results about the mean amounts to about 10% of the value. The progressive saturation method is open to the objections mentioned above. It is usually found advisable to take all the relaxation time measurements in one continuous sequence, but because of the necessary change from liquid hydrogen to liquid nitrogen between 45°K and 62°K, this was not possible with this cryostat.

Because of these factors, not too much significance should

be attached to the fact that the value at 62°K is higher than that at 40°K. Of more importance is the shape of the two parts of the curve: between 20°K and 45°K the spin-lattice relaxation time does not vary much with temperature, but between 60°K and 100°K it becomes very temperature-dependent. This point will be further discussed in the following section.

#### 4.4.6 Discussion

The value of the second moment of n-octane at 120°K,  $18.8 \pm 0.4$  gauss<sup>2</sup>, has to be compared with the theoretical value, as calculated from equation (8).

The intramolecular contribution can be calculated exactly using the molecular configuration detailed in section 4.4.3. This gives a value of 20.4 gauss<sup>2</sup>. Calculation of the intermolecular second moment, however, presents more difficulty, as there is some uncertainty about the exact positions of the protons in neighbouring methyl groups. The long spacing between the molecules of n-octane is given as 14.0 Å by Müller (1930). Taking this value, with the molecules arranged with their long axes parallel to the c-axis of the unit cell, we find

that the separation between protons in the methyl groups at the ends of adjacent molecules is only 0.55 Å. This is a very short distance of approach and we should expect the molecules to act in such a way as to relieve this. Müller suggests various methods by which this could happen. The molecules may shorten or may tilt relative to the base of the unit cell, there may be a rearrangement of the end groups, or, of course, there may be a combination of these effects. The exact positions of the protons in the end methyl groups are therefore uncertain. The interactions between these methyl groups will very probably dominate the value of the intermolecular second moment, and so this cannot be evaluated exactly.

However, an estimate of the intermolecular second moment can be made. Müller (1930) has shown that the a and b dimensions of the unit cell for molecules between  $C_5H_{12}$  and  $C_{30}H_{62}$  are effectively constant, and may be taken equal to the value found for  $C_{29}H_{60}$ . We may consider only the interactions between a proton in one of the central methylene groups of one molecule, and all the protons in the other molecules in the same and adjacent unit cells. If we consider such interactions as typical, we may compute the intermolecular

contribution. The second moment depends on a term  $\sum r_{jk}^{-6}$  and so only nearest neighbours are important: for interproton distances less than 5 Å, the interactions may be treated exactly, while for distances greater than this, the summation may be replaced by an integral, it being assumed that the more distant protons are evenly distributed in space. For sufficiently long molecules, we need not consider interactions with protons of molecules in layers above or below the typical molecule, as the separations will be greater than 5 Å.

Andrew and Eades (1953b) applied this method to n-hexane. Taking a reasonable lattice concentration, they estimated the intermolecular contribution at 120°K to be 9.6 gauss<sup>2</sup>. This method will be more exact for longer molecules, and so this value is applicable to n-octane. An uncertainty of  $\pm 1.5$  gauss<sup>2</sup> should be sufficient.

The total second moment at 120°K is thus 30.0  $\pm$  1.5 gauss<sup>2</sup>. The experimental value at this temperature is 18.8  $\pm$  0.4 gauss<sup>2</sup>, itself less than the rigid intramolecular contribution. This difference of 11.2 gauss<sup>2</sup> may be explained by molecular motion.

The two most likely forms of motion which we must consider are

(i) rotation of the molecules about their long axes.

(ii) rotation of the methyl groups about the end C-C axes.

(i) The theoretical value for the intramolecular contribution to the second moment for this motion can be calculated, using the theory outlined in sections 2.2 and 4.2.4. Fortunately the most important part of the second moment - the intramolecular contribution - is the part known exactly. The value found is  $5.5 \text{ gauss}^2$ . The reduction of  $14.9 \text{ gauss}^2$  is too great, being by itself more than the discrepancy of  $11.2 \text{ gauss}^2$ . The appropriate reduction in the intermolecular contribution will reduce the total second moment still further and so it is unlikely that this type of motion is in fact occurring.

(ii) The intramolecular contribution to the second moment when rotation of the methyl groups takes place can be calculated by another method. Since only part of each molecule moves, both  $r$  and  $\theta$  vary, and this calculation is similar to that for the reduction of the intermolecular second moment (Andrew and Bades 1953b). The contribution from the interactions of the protons of each methyl group amongst themselves



is reduced by a factor of four, as each interproton axis is perpendicular to the axis of rotation (equation 16). This calculation gives a value of  $14.0 \text{ gauss}^2$  for the intramolecular part, a reduction of  $6.4 \text{ gauss}^2$ . The value of the intermolecular contribution must now be reduced by a half to  $4.8 \text{ gauss}^2$ . This reduction is reasonable as only a third of the protons in each molecule are involved in the rotation. An accurate value for the intermolecular contribution cannot be found, because of the uncertainty in the positions of the methyl group protons. However, it appears probable that this is in fact the form of molecular motion occurring.

The fine structure found in the absorption line is probably produced by the methyl groups. Andrew and Bersohn (1950) have calculated the spectrum expected from a system of three protons, situated at the corners of an equilateral triangle, reorienting about an axis. For the special case where the axis of reorientation is perpendicular to the plane of the triangle, the spectrum consists of a central line, and a pair of lines placed symmetrically about the central line. For a polycrystalline specimen, considering

the interactions from neighbours, the spectrum will contain a small central peak, being shown as a secondary maximum and minimum on the derivative curve; this is the form of structure observed. Of the total intramolecular contribution of  $14.0 \text{ gauss}^2$ ,  $10.4 \text{ gauss}^2$  is provided by mutual interactions between the methylene groups, and this will tend to mask the fine structure. The central peak will, therefore, be small.

The spin-lattice relaxation time measurements give some additional information about the reorientation process.

Hoembergen, Purcell and Pound (1948) have shown that molecular reorientation, when it occurs in a solid, provides the most powerful relaxation mechanism. On this basis, assuming random motion, they derive an general expression for the spin-lattice relaxation time, for nuclei with spin  $I = \frac{1}{2}$ ,

$$\frac{1}{T_1} = \frac{3}{2} \gamma^4 \hbar^2 I(I+1) [J_1(\nu_0) + \frac{1}{2} J_2(2\nu_0)]$$

where  $J_1$  and  $J_2$  are the intensities of the Fourier spectra of the position coordinates concerned. They further assumed that the motion could be adequately described by a single correlation time

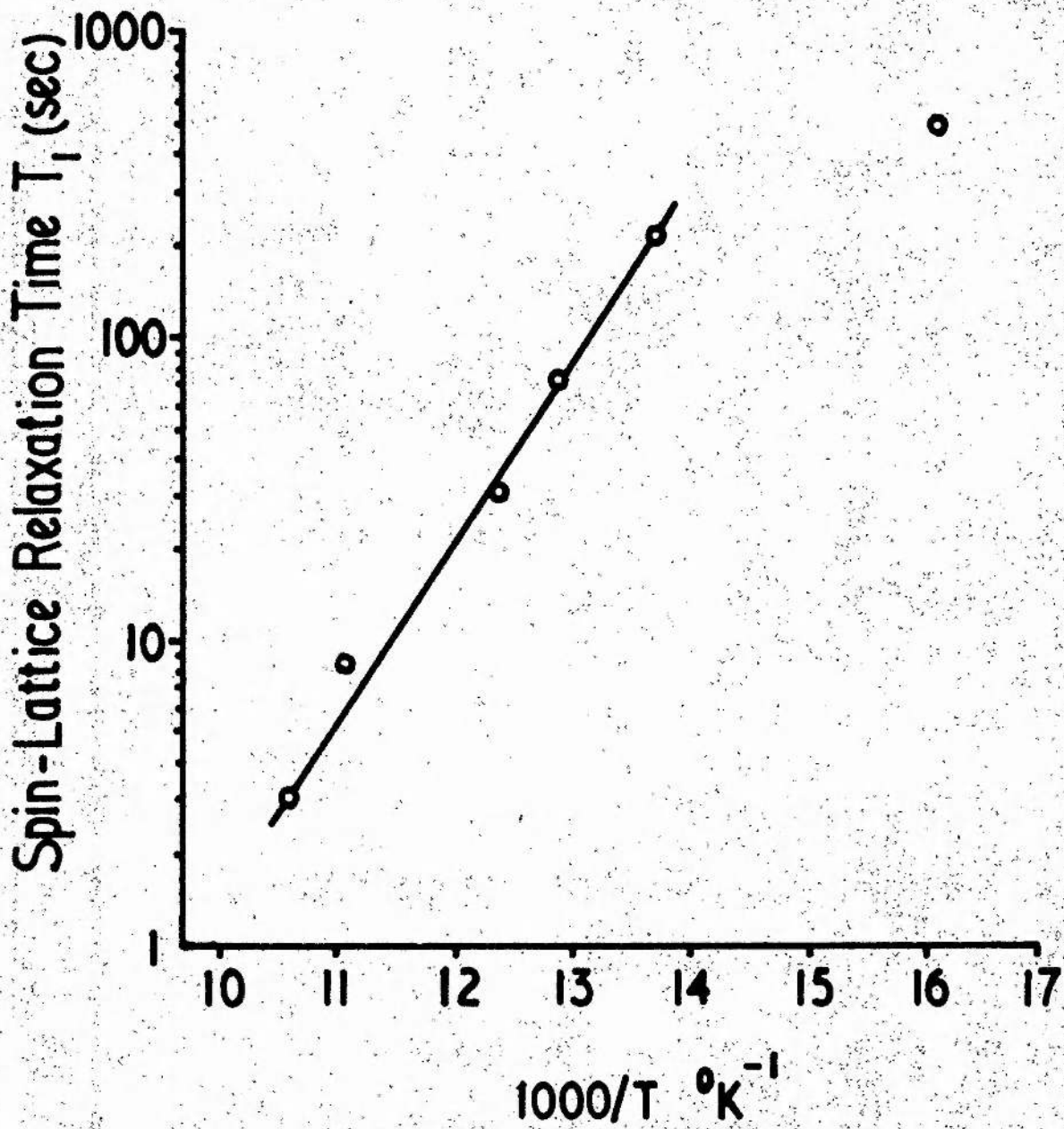


FIGURE 13

$\tau_c$ , and that only one neighbour was important in the relaxation mechanism. The above general relation then simplifies to

$$\frac{1}{T_1} = C \left[ \frac{\tau_c}{1 + \omega^2 \tau_c^2} + \frac{2\tau_c}{1 + 4\omega^2 \tau_c^2} \right]$$

where  $\omega/2\pi$  is the radiofrequency used, and  $C$  is a constant. If

$\omega\tau_c \gg 1$ , this simplifies further to

$$T_1 = \frac{2\omega^2 \tau_c}{3C}$$

Provided that  $\tau_c$  can be expressed in the form  $\tau_c = \tau_0 e^{V_0/RT}$ , where

$V_0$  is the height of the barrier restricting the rotation, and  $R$  is the gas constant, then we may write

$$T_1 = \frac{2\omega^2 \tau_0}{3C} e^{V_0/RT}$$

and so

$$\log T_1 = \log \frac{2\omega^2 \tau_0}{3C} + \frac{V_0}{RT} \log e \quad (17)$$

If this theory is a fair description of the actual relaxation mechanism, a plot of  $\log T_1$  against the reciprocal of the absolute temperature should give a straight line of slope  $V_0/R$ . For values of  $T$  between 62°K and 94°K the graph is shown in figure 13. These values of  $\log T_1$  do lie on a straight line, except for the value at  $T = 62^\circ\text{K}$ . The lower temperature values do not lie on this line, and will be discussed later.



The slope of this line gives a value for  $V_0$  of 2600 cal/mole. The accuracy of this value will not be high, because of the many assumptions made in the derivation of equation (17), and because of the possible errors in the relaxation time measurements themselves. This value may, however, be compared with the barrier heights determined for other members of the series of n-paraffins. The values for the two lowest members of the series, ethane and propane, are 2750 cal/mole, and 3300 cal/mole respectively (Aston 1951). It is believed (Pitzer 1951) that the barrier to rotation is principally due to interactions between the methyl groups and other hydrogen atoms in the same molecule. Furthermore, the interactions are repulsive: we should expect the methyl groups in the ethane molecule to be "staggered". French and Rasmussen (1946) have developed a method of calculating these barrier heights. They regard the barrier at a methyl group as being due to the sum of the contributions from interactions with groups on the other end of the rotational axis. For example the barrier of 2750 cal/mole in ethane may be considered as three times the barrier due to a single hydrogen at the other end of the molecule. The minimum distance of approach of a hydrogen nucleus of the methyl



group to any hydrogen nucleus on the opposing group, is then a convenient measure of the interaction. The interaction therefore falls off with distance, and the barrier will in general be determined by the nearest neighbours. The value for n-octane should be approximately the same as for ethane, propane etc. as the addition of methylene groups will have a very slight effect on the barrier height. The experimental value for n-octane, 2600 cal/mole, is therefore of the correct order of magnitude. This agreement is quite gratifying, considering the assumptions made in the derivation of equation (17).

In order to explain the relaxation times in the temperature range 20°K to 40°K, we must examine more closely the barrier hindering the rotation, and the actual energy levels.

In the case of a symmetric group such as a methyl group, the barrier must consist of a set of equally spaced minima. The potential function  $V$  may then be expanded as a Fourier series

$$V = \sum_{\gamma} \frac{V_{\gamma}}{2} (1 - \cos \beta \gamma \phi)$$

where  $\phi$  is the angular coordinate which defines the orientation of the methyl group relative to the neighbouring methylene groups. It is

usually a sufficiently good approximation to take only the first term of the series,

$$V = \frac{V_0}{2} (1 + \cos 3\theta)$$

The torsional oscillation energy levels  $E_i$  then lie in these minima. Each energy level is split into two sublevels, one of which is doubly degenerate (Powles and Gutowsky 1954). The splitting  $\Delta\nu_i$  between the sublevels is small compared to the separation between adjacent energy levels. It may be shown that  $\Delta\nu_i$ , in the appropriate units, is just the frequency of barrier penetration (Byring, Walter and Kimball, 1944, p310).  $\Delta\nu_i$  increases with  $E_i$ ; that is as the energy increases so does the rate of tunnelling through the barrier.

It is of interest to examine the approximate rate of tunnelling expected. The barrier heights for ethane and n-octane should be about equal, and so we may use experimental results obtained for ethane. Kistiakowsky, Lacher and Stitt (1939) showed that the splitting of the first level of ethane,  $\Delta\nu_1$ , is just  $0.4 \text{ cm}^{-1}$ ; this is equal to  $7.9 \times 10^{-17}$  ergs, which corresponds to a frequency of  $1.2 \times 10^{10} \text{ sec}^{-1}$ , a very high tunnelling frequency. The average

line width expressed as a frequency is of the order of 100 Kc/s; this process could, therefore, very easily produce the absorption line narrowing found for this hydrocarbon.

Suppose we cool the n-octane sample to a temperature such that almost all the molecules are in the lowest energy level  $E_0$ . Because the splitting of the sublevels is much less than the separation between adjacent levels, the sublevels will be almost equally populated. When most of the molecules are in the lowest level  $E_0$ , the rate of tunnelling will be  $\Delta\nu_0$ , and we should not expect the spin-lattice relaxation time to vary much with temperature. As the temperature increases however, more molecules are raised to the higher levels  $E_1$ ,  $E_2$ ,  $E_3$  and so on; since  $\Delta\nu_1 < \Delta\nu_2 < \Delta\nu_3$  etc. the rate of tunnelling increases and we should expect the relaxation time to become strongly temperature-dependent.

Kistiakowsky et al have shown that the first excited level for ethane is  $275 \text{ cm}^{-1}$  above the ground level. This separation corresponds to an energy of  $5.5 \times 10^{-14}$  ergs. Suppose we have only two energy levels  $E_0$  and  $E_1$ . The ratio of the populations of these two levels is then given by

$$\begin{aligned}\frac{n(E_0)}{n(E_1)} &= \frac{1}{3} \cdot e^{5.5 \times 10^{-14}/kT} \\ &= \frac{1}{3} e^{400/T}\end{aligned}$$

This population ratio at various temperatures is shown in the following table:

Temperature °K	$n(E_0)/n(E_1)$
20	$\frac{1}{3} e^{20} = 2.7 \times 10^8$
40	$\frac{1}{3} e^{10} = 9.5 \times 10^3$
60	$\frac{1}{3} e^{6.6} = 2.4 \times 10^2$
80	$\frac{1}{3} e^5 = 50$

There is thus a large variation in the population ratio over this temperature interval, and the fact that the spin-lattice relaxation time becomes strongly temperature-dependent at about 60°K is not surprising on the basis of this rather crude picture. Above 60°K sufficient molecules are in the upper energy levels to permit the use of the relation  $\tau_c = \tau_0 e^{V_0/kT}$ .

We can also see that an extremely low temperature would be necessary to "freeze-out" this reorientation of the methyl groups. The temperature would have to be so low that practically all the

molecules were in the lower sublevel of the lowest energy state.

The splitting  $\Delta\nu_0$  of the lowest state will be smaller than  $\Delta\nu_1$

for ethane. We have shown this to be  $7.9 \times 10^{-17}$  ergs, which,

when divided by the Boltzmann constant  $k$ , corresponds to a

temperature of 0.5°K.



4.5 CYCLOOCTATETRAENE ( $C_8H_8$ )

CYCLOOCTATETRAENE (C<sub>8</sub>H<sub>8</sub>)

4.5.1 Introduction

Many investigations of the molecular configuration of cyclooctatetraene have been made, using the techniques of infra-red and Raman spectroscopy, and of electron diffraction. In view of the conflicting results given by these experiments it was decided to study the nuclear resonance absorption spectrum of solid cyclooctatetraene. As was shown in section 2.2, the second moment of the absorption spectrum depends on the positions of the protons; each configuration will give a different value for the second moment, and an experimental study of the absorption spectrum might be able to differentiate between the various possible molecular structures.

The specimen examined was supplied by British Oxygen Research and Development Ltd. The minimum purity quoted was 99.7 mole per cent, as determined from the refractive index.

Cyclooctatetraene reacts readily with oxygen. The specimen supplied was freshly distilled and sealed in the ampoule under nitrogen. It was transferred to the 6 mm Pyrex tube and sealed under vacuum.

#### 4.5.2 Thermal Data

The heat capacity from 15°K to the melting point, heats of fusion and vapourisation, vapour pressure and entropy of cyclooctatetraene have been measured by Scott, Gross, Oliver and Huffman (1949). They found no evidence of a transition in the specific heat within these temperature limits. Values quoted are:

Melting point	268.478°K
Heat of fusion	2694.6 cal/mole
Heat of vapourisation	10,300 cal/mole

However, Pink and Ubbelohde (1948) have reported a specific heat transition in the neighbourhood of 98°K, with a heat of transition of approximately 400 cal/mole. They also noted that the crystals changed suddenly from white to yellow as the substance was warmed through this temperature. In view of this, Scott et al made a specially detailed study of the specific heat in this temperature region, and found no evidence of a transition, nor of a sudden colour change.

Pink and Ubbelohde had not sufficient material at their disposal to permit exhaustive purification, and they admit that it is possible that the colour change is due to the freezing-out of impurities which

remained in solid solution at the higher temperatures. This freezing-out might cause the soft crystals to break up, increasing the apparent whiteness. However, more recent measurements by McDonnell, Pink and Ubbelohde (1950) again show the presence of a transition in susceptibility and colour at this temperature.

The specimen examined here showed no sudden colour change. When immersed in liquid nitrogen the crystals were very pale yellow. As the sample warmed slowly, the colour deepened steadily, until, at the melting point, the cyclooctatetraene was a strong yellow.

Pink and Ubbelohde (1948) quote thermal data given by Reppe

Boiling point at 760 mm =  $142 - 143^{\circ}\text{C}$

Mean latent heat of vapourisation over

this temperature interval =  $9.86 \text{ K cal/mole}$

Entropy of vapourisation at melting point =  $25.7 \text{ cal/deg.}$

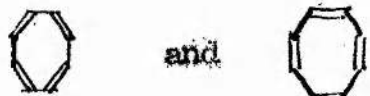
#### 4.5.3 Crystal structure

The crystal structure of solid cyclooctatetraene at  $-7^{\circ}\text{C}$  has been determined by Kaufman, Fankuchen and Mark (1947) using X-ray methods. They found the crystal to be face-centred orthorhombic,

with unit cell dimensions  $a = 7.76 \text{ \AA}$ ,  $b = 7.80 \text{ \AA}$ ,  $c = 10.66 \text{ \AA}$ . The crystal belongs to the space-group  $Aba \left( O_{2v}^{17} \right)$ . The  $c$ -axis of the unit cell is a two-fold axis of symmetry, and thus the molecular configuration must possess at least a diad axis. There are four molecules per unit cell: the centres of gravity of these molecules have coordinates  $(0, 0, 0)$ ,  $(0, \frac{1}{2}, \frac{1}{2})$ ,  $(\frac{1}{2}, 0, \frac{1}{2})$  and  $(\frac{1}{2}, \frac{1}{2}, 0)$ , according to the International Tables for X-ray Crystallography.

The orientation of the molecules with respect to the  $c$ -axis is not known. If there were no interactions between molecules, we should expect an angle of  $45^\circ$ . However, mutual repulsions of the molecules will reduce this angle and a value of  $40^\circ$ , as found for benzene (Cox 1932) seems reasonable.

#### 4.5.4 Molecular Structure

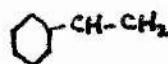
On the basis of the chemical formula, we might expect cyclooctatetraene to have a molecular structure similar to that of benzene  $C_6H_6$ : some authors have termed it "octabenzene". This would mean an aromatic molecule, resonating between the two molecular structures . The values given for the latent heat of vapourisation, and for the entropy of vapourisation at



the boiling point (section 4.5.2) may be compared with the corresponding values of  $\Delta H = 7.0$  kcal/mole and  $\Delta S = 19.75$  cal/deg/mole for benzene.


Values of the resonance energy for the two substances, however, show a greater difference. By resonance energy we mean the energy stabilising the system on account of the resonance between the two structures. Pink and Ubbelohde (1948) have computed the resonance energy. They showed that the heat of formation of cyclooctatetraene from atoms of the constituent elements is  $-1358.1$  kcal/mole; the sum of the bond energies, assuming a single structure of four double and four single bonds for the molecule in its normal state is  $1332.8$  kcal/mole. The difference between these two energies ( $25.3$  kcal/mole) is the resonance energy. This value may be compared with the corresponding  $39$  kcal/mole for benzene (Pauling 1948). While the resonance energy of cyclooctatetraene is less than that of benzene, it is not unusually high for an aliphatic type of structure, but it does suggest the possibility that cyclooctatetraene may have some aromatic character. However, the cyclooctatetraene ring does not possess the great stability of the benzene ring: from the point of

view of energy content it is less stable than its isomer styrene

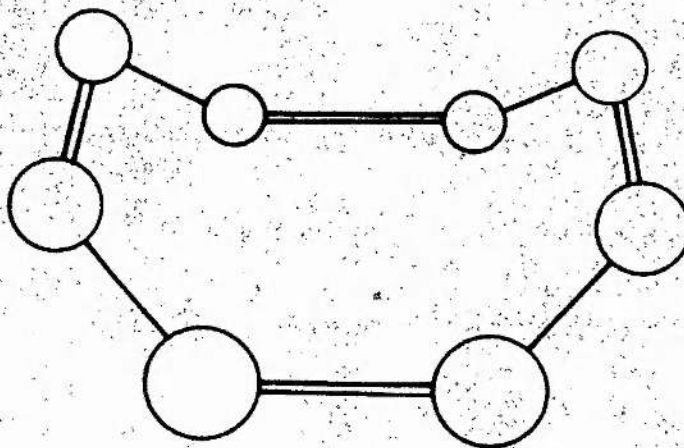


by 34 kcal/mole (Frosen, Johnson and Rossini 1947). In

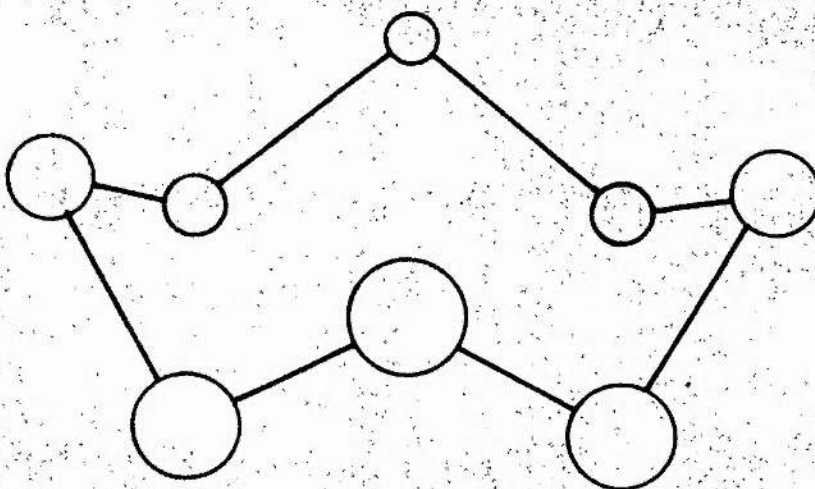
many reactions it shows a markedly unsaturated character.

Measurement of the diamagnetic susceptibility should theoretically provide a more definite test for the presence of aromatic character than resonance energy. An aromatic molecule possesses essentially a "pool" of electrons, giving a substantially higher diamagnetism per electron than in the case of bound electrons. Pink and Ubbelohde (1948) have measured the diamagnetic susceptibility of cyclooctatetraene and obtained good agreement with theoretical values for a system of conjugated double and single bonds. Such a result could, however, be obtained from a system, essentially aromatic but with a very small amount of a paramagnetic "diradical"  present. An impurity concentration as low as  $6 \times 10^{-5}\%$  would be sufficient to give this result. We should then expect the susceptibility of such a system to alter with temperature. The results of McDonnell, Pink and Ubbelohde (1950) show that this is not so, and strengthen the evidence for a system of conjugated double and single bonds.

$D_{2d}$



$D_{4d}$



$D_4$

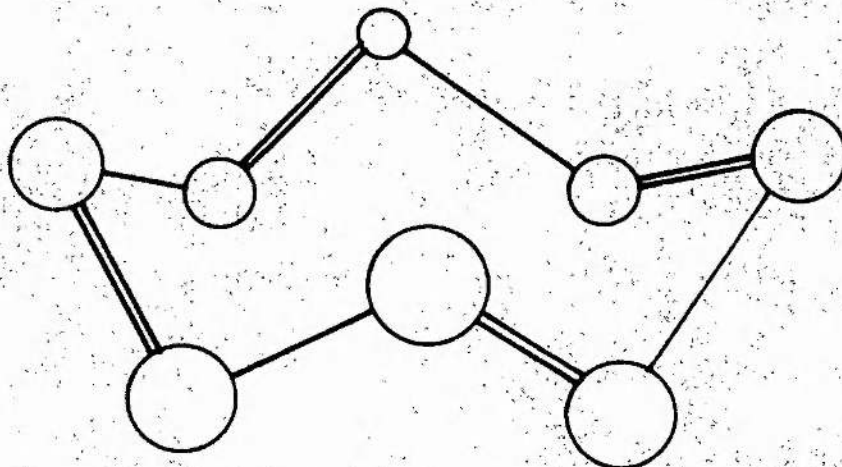


FIGURE 14.

Lippincott and Lord (1946) studied the Raman spectrum of liquid cyclooctatetraene. They concluded that:

(i) the molecule cannot have cubic symmetry ( $O_h$ ), or planar symmetry with an eight-fold axis of symmetry ( $D_{8h}$ ), as the number of polarised lines is too large

(ii) the molecule cannot have two different geometrical forms because the spectrum is too simple

(iii) all the hydrogen atoms are equivalent

(iv) the molecule contains no triple bonds, and no  $=CH_2$  or  $-CH_3$  groups

(v) the molecule possesses a multiple axis of symmetry.

These authors located a strong polarised line at a C = C bond frequency. They concluded that a puckered eight-membered ring with alternate double and single bonds ( $D_4$  symmetry) best fitted with the observed Raman spectral lines. This molecular configuration is illustrated in figure 14, and is usually termed a "crown" structure.

An electron diffraction analysis of the vapour led Bastiansen,



Hassel and Langseth (1947) to an entirely different conclusion. They found that all the carbon bonds are equivalent, and that the bond angles are  $120^\circ$  as in the case of the benzene molecule. The C - C bond length they found to be approximately 2% greater than the corresponding bond in benzene. Satisfactory agreement between theory and experiment was obtained only for a molecule consisting of a puckered ring with equivalent bonds ( $D_{4d}$  symmetry). This molecular configuration is also shown in figure 14, and this too is a "crown" structure.

These authors also reinvestigated the Raman spectrum of cyclooctatetraene. They disagreed with Lippincott and Lord (1946) over several frequencies, and again find evidence in support of a  $D_{4d}$  model.

Flett, Cave, Vago and Thompson (1947) have further investigated the structure. They measured the infra-red spectrum of the vapour and of the liquid, and the Raman spectrum of the liquid. The Raman intervals obtained agreed quite well with those reported by Lippincott and Lord; some of the weaker displacements, found by these authors were not observed however. The results were considered in terms of



five different molecular models: a planar molecule with an eight-fold axis of symmetry ( $D_{8h}$ ); a planar molecule with a four-fold axis ( $D_{4h}$ ); a "tub" form with double and single bonds ( $D_{2d}$ ); puckered ring molecule with double and single bonds ( $D_4$ ); puckered ring molecule with equivalent bonds ( $D_{4d}$ ). These authors report that although no clear decision seemed possible, they were inclined to think that the experimental results were in best agreement with the non-planar "tub" ( $D_{2d}$ ) structure (figure 14).

Rather more definite evidence in favour of the "tub" configuration came from the X-ray analysis by Kaufman, Fankuchen and Mark (1948). These authors found that only this form with alternating double and single bonds, fitted the experimental results. They also measured the bond lengths, and found them to be typically aliphatic. The double bond length was 1.34 Å, and the single bond length 1.54 Å; the C=C-C angle was 125°. The diad axis of symmetry, demanded by the space-group  $Aba$ , must then pass through the single bonds.

Lippincott, Lord and McDonald (1948) extended the work done previously by the first two authors (1946). They studied the

infra-red and Raman spectra of cyclooctatetraene ( $C_8H_8$ ) and of the completely deuterated molecule  $C_8D_8$ , prepared by the polymerisation of heavy acetylene. The Raman spectrum of  $C_8H_8$  entirely confirmed their previous results. From the infra-red and Raman spectra of both  $C_8H_8$  and  $C_8D_8$ , these authors find convincing support for the  $D_{4h}$  structure.

Coulson and Moffitt (1949) have made a theoretical study of several strained hydrocarbons including cyclooctatetraene. They conclude that  $D_{2d}$  is a more likely structure than  $D_{4h}$ ; energetically the  $D_{2d}$  is more stable than the  $D_{4d}$  by 5 eV per molecule. These authors, however, have not considered the alternative crown configuration with double and single bonds ( $D_4$ ) favoured by Lippincott and Lord. The bond lengths in the  $D_{2d}$  would alternate, being about 1.54 Å, and 1.34 Å, in agreement with the results of Kaufman et al (1948).

The Raman spectrum has been investigated also by Saksena and Narain (1950). The spectrum obtained makes them inclined to favour the  $D_{4d}$  structure, although the  $D_{4h}$  cannot be excluded altogether.

Lippincott, Lord and McDonald (1950) find fault with the results and reasoning in this paper; these authors again give strong support to a  $D_4$  molecule.

Lippincott and Lord (1951) have investigated the thermodynamic functions of cyclooctatetraene. They conclude that the close similarity between the vibrational spectra of the  $D_{4d}$  and  $D_{2d}$  configurations makes impracticable any distinction between the two structures by methods of statistical mechanics such as a comparison of calculated and experimental entropy values.

Karle (1952) has made another analysis of the electron diffraction of cyclooctatetraene. From the radial distribution curve computed, she concluded that the "tub" ( $D_{2d}$ ) form was most likely, with the oblique C-C bonds longer than the horizontal ones. However, the maxima in the distribution curves occurred at the same positions for both "crown" and "tub" forms; only the shape of the maxima differentiated between the two. The single and double bond lengths were respectively 1.50 and 1.35 Å; however, reasonable agreement was obtained with the radial distribution curves for a common bond length of 1.42 Å.

Another theoretical investigation has been made by Person, Pimentel and Pitzer (1952). They favour double and single bonds, rather than an equivalent bond, and try to distinguish between the two forms then possible. They take known potential energy functions from related molecules, and obtain complete agreement with the  $D_{2d}$  molecule. The  $D_4$  configuration is more difficult to understand on the basis of the same potential functions.

Saksena and Bhatnagar (1953) have revised the calculations of Saksena and Narain (1950), for the  $D_4$  structure, and have made new calculations for the  $D_{2d}$ . They conclude that pure double and single bonds do not exist in the molecule.

Since the completion of the work reported here, Bastiansen, Hedberg and Hedberg (1957) have reported another electron diffraction analysis of the cyclooctatetraene structure, using highly refined diffraction techniques. They support definitely the  $D_{2d}$  configuration. However, the radial distribution curves drawn for the diffraction are again very similar for both the  $D_{2d}$  and  $D_4$  models: the first two peaks ( $r < 2.75 \text{ \AA}$ ) are exactly similar but the third peak shows a slight distinction, enabling these authors to decide in

favour of the  $D_{2d}$ .

Summarising, we see that the molecular structure of cyclooctatetraene is a very controversial subject, each of the three configurations  $D_4$ ,  $D_{4d}$  and  $D_{2d}$  having its supporters. It appears that there is too great a similarity between the various vibrational spectra, and between the radial distribution curves for electron diffraction for the three configurations to enable a quite definite determination of the structure to be made by these methods. Even the most refined technique adopted by Bastiansen, Hedberg and Hedberg (1957) shows only a small theoretical distinction between the models. It will be shown in section 4.5.6 that nuclear magnetic resonance provides a much greater theoretical difference between the three forms, and thus makes a determination of the structure much more definite.

All authors agree, however, in rejecting the plane molecule, exactly similar to benzene. If cyclooctatetraene were aromatic, the undistorted bond angles would be  $120^\circ$ ; in a regular octagon the angles would be  $135^\circ$ . The strain needed to distort the bond angles by this  $15^\circ$ , would probably be much greater than the resonance



energy acquired by assuming the planar structure, and would make this configuration extremely unlikely.

#### 4.5.5 Absorption Spectrum

The first derivative of the absorption curve was plotted at 20°K, 90°K and 235°K, using the lock-in amplifier, and recording meter. The second moment of the absorption spectrum was calculated, using equation (14) and corrected, as usual for the broadening due to the field modulation (equation 15). Mean values found for the second moment are:

	Second Moment ( $G^2$ )
20°K	9.5 ± .5
90°K	9.4 ± .4
235°K	7.9 ± .2

Quoted errors are once again the standard deviations.

The particular temperature at which the last set of results were taken (235°K) has no special significance. With the gas-flow method of cooling (section 3.4) it is difficult to attain a particular desired temperature: it is, however, very easy to maintain the

temperature reached. This temperature of 235°K has the advantage that it is well below the melting point, so that there is no risk of the specimen accidentally melting with possible subsequent supercooling, and yet is sufficiently near the temperature at which the crystal structure was determined (-7°C) to render unnecessary any correction for lattice contraction in the calculation of the second moment.

The strength of the signal obtained from cyclooctatetraene was considerably less than for the other hydrocarbons studied; there was a corresponding decrease in the signal-to-noise ratio, necessitating a fairly large modulation and a long time constant. The poor signal strength was due to the relatively low density of protons in the sample: the ratio (number of protons)/(number of carbon atoms) is equal to unity for cyclooctatetraene, whereas for cyclopentene and n-octane it equals 8/5 and 18/8 respectively.

The second moment values show no great variation in the temperature interval studied, suggesting that the lattice is effectively rigid at these temperatures. The increase which does occur in the second moment as the temperature is lowered may be

explained simply on the basis of thermal contraction of the lattice; this will be demonstrated in the following section:

#### 4.3.6 Discussion

The experimental value for the second moment at 235°K,  $7.9 \text{ G}^2$ , must be compared with the theoretical values for various molecular models. Previous investigations (section 4.5.4) have favoured any of the three configurations  $D_4$ ,  $D_{4d}$  or  $D_{2d}$ . These structures are all discussed theoretically; to make the investigation more complete, we also treat the plane case. The three structures  $D_4$ ,  $D_{4d}$ ,  $D_{2d}$  are illustrated in figure (14); only the carbon atoms are shown.

It is again convenient to divide the second moment into intramolecular and intermolecular parts. The four molecular models are considered separately:

##### (1) plane molecule ( $D_{8h}$ )

This structure is in the form of a regular octagon, with bond angles of  $136^\circ$ . Bastiansen et al (1947) show that in their puckered ring molecule equivalent C-C bond is about 2% greater than in benzene.

Brockway and Robertson (1939) find this bond length in benzene to be 1.39 Å; a length of 1.42 Å is thus assumed for cyclooctatetraene. For the carbon-hydrogen bond length we assume 1.08 Å, intermediate between 1.09 Å for  $\text{-C-H}$  and 1.07 Å for  $\text{=C-H}$  (Herzberg 1945). Using this geometry the coordinates for all the protons were calculated, and, using equation (3), the intramolecular contribution to the second moment evaluated.

(ii) puckered ring with equivalent bond ( $D_{4d}$ )

The same bond lengths were taken as for the plane molecule. The  $\text{C-C-C}$  angle was assumed to be  $120^\circ$  (Pastlansen et al 1947); in all models the  $\text{=C-H}$  bond was assumed to lie in the plane defined by the three neighbouring carbon atoms, and to bisect the  $\text{C-C-C}$  angle.

(iii) puckered ring with double and single bonds ( $D_4$ )

Typically aliphatic bond lengths were assumed:  $\text{C-C} = 1.54$  Å,  $\text{C=C} = 1.34$  Å; the  $\text{C-C-C}$  angle was assumed  $125^\circ$  as in the "tub" form.

(iv) "tub molecule with double and single bonds ( $D_{2d}$ )

The same bond lengths and angles were used as in the  $D_4$  structure,

i. e. C-C = 1.54 Å, C=O = 1.31 Å, C=C-C = 125° (Kaufman et al 1948).

The intermolecular contribution to the second moment was also computed for each of the four molecular configurations. The unit cell dimensions measured by Kaufman et al (1947) were used; the lattice contraction occurring between 235°K, the temperature at which the second moment was measured, and 265°K, at which the X-ray investigation was made, is negligible.

The calculation of the intermolecular second moment is necessarily tedious, because of the large number of interproton distances involved. In each case, the nearest molecules were treated exactly; for molecules whose centres were more distant than 8 Å, it was assumed that all the nuclei were at the centre of gravity of the molecule when treating the interactions. Symmetry in the molecules simplified the calculation greatly. Because we are computing a term  $\sum r^{-6}$ , the interaction falls off rapidly with distance, and so only molecules which are relatively close need be considered.

The theoretical second moments for cyclooctatetraene are:



	Intramolecular Second Moment ( $G^2$ )	Intermolecular Second Moment ( $G^2$ )	Total ( $G^2$ ).
Plane	5.75	5.47	11.22
$D_{4d}$	1.99	7.05	9.04
$D_4$	2.58	7.75	10.13
$D_{2d}$	2.99	5.00	7.99

The mean experimental value was  $7.9 \pm 0.2$  gauss<sup>2</sup>. We see, therefore, that this method distinguishes quite definitely in favour of the  $D_{2d}$  "tub" molecule, with conjugated double and single bonds. This is in agreement with the very recent electron diffraction of Eastmann et al (1957), referred to in section 4.5.4. In contrast to the predictions of infrared spectroscopy, and of electron diffraction, nuclear magnetic resonance provides a large theoretical distinction between the various possible configurations, enabling a definite conclusion to be reached.

The large theoretical distinction in this case is quite fortunate, and need not have occurred. For this reason it is advantageous, whenever possible, to use a single crystal when making structural determinations by means of nuclear resonance. Van Vleck's equation for the second moment (equation 7) contains both  $\tau_{jk}$  and  $\theta_{jk}$ ; by

altering the orientation of the crystal in the magnetic field,  $\theta_{jk}$  is altered, and the second moment may be anisotropic. An example of this type of work is the determination of the wholly planar nature of the urea molecule by Andrew and Hyndman (1953).

Finally, we must show that the second moment values found at the lower temperatures can in fact be explained solely on the basis of thermal contraction of the lattice. The actual thermal expansion of cyclooctatetraene is unknown, but may be estimated. Since the unit cell is orthorhombic, the thermal expansion coefficient will probably be different for each of the three principal directions; however, we consider here a 2% average linear contraction. This is of a reasonable magnitude, being comparable with known contractions for benzene (summarised by Rades 1952) and the n-paraffins (Müller 1930). If we make the reasonable assumption that the molecular bond lengths are not shortened, the  $D_{2d}$  molecular configuration then gives a total second moment of 9.8 gauss<sup>2</sup>. The observed increase in second moment values can thus be explained by this mechanism alone.

5. SUMMARY

5. SUMMARY

The nuclear resonance absorption spectrum of several hydrocarbons has been studied at temperatures down to 20°K, using the bridge method of detection. A special cryostat was constructed for use with liquid hydrogen.

In the case of cyclopentene, experimental evidence has been found in favour of a non-planar molecule, rotating about an axis perpendicular to the plane defined by four of the carbon atoms. This motion starts near 87°K, the temperature of the reported specific heat transition. At 124°K, the molecules appear to diffuse through the lattice, so that at 128°K, 10° below the melting point, the line width is less than the field inhomogeneity.

Measurements of the second moments of n-pentane, n-hexane and n-octane indicate reorientation of the methyl groups about the end C-C axes, even at 20°K. An approximate value for the height of the barrier restricting the rotation in the n-octane molecule has been determined from the spin-lattice relaxation time measurements.

Second moment measurements on cyclooctatetraene have provided

strong evidence in favour of a "tub" ( $D_{2d}$ ) structure of the molecule, with conjugated double and single bonds.

In conclusion, the author would like to express his sincere thanks to Dr. F. A. Rushworth for his encouragement and guidance during the course of this work, to Professor J. F. Allen, F.R.S. for his interest and advice, and to Mr. J. Gerrard for assistance with the photography.



6. REFERENCES

6. References

Anderson, H.L. (1949) Phys. Rev. 76, 1460.

Anderson, P.W. (1954) J. Phys. Soc. Japan 2, 316.

Andrew, E.R. (1950) J. Chem. Phys. 18, 607.

Andrew, E.R. (1953) Phys. Rev. 91, 425.

Andrew, E.R. (1954) Defects in Crystalline Solids: report of Bristol Conference of the Physical Society.

Andrew, E.R. (1955) Nuclear Magnetic Resonance. Cambridge University Press.

Andrew, E.R. (1957) Private communication.

Andrew, E.R. and Bersohn, R. (1950) J. Chem. Phys. 18, 159.

Andrew, E.R. and Eades, R.G. (1953a) Proc. Phys. Soc. Lond. A66, 415.

Andrew, E.R. and Eades, R.G. (1953b) Proc. Roy. Soc. A216, 398.

Andrew, E.R. and Finch, N.D. (1957) Proc. Phys. Soc. Lond. B70, 980.

Andrew, E.R. and Hyndman, D. (1953) Proc. Phys. Soc. Lond. A66, 1187.

Andrew, E.R. and Rushworth, F.A. (1952) Proc. Phys. Soc. Lond. B65, 801.

Aston, J.G. (1951) Disc. Faraday Soc. 10, 75.

Bastiansen, O., Hassel, O. and Langseth, A. (1947) Nature 160, 128.

Bastiansen, O., Hedberg, L. and Hedberg K. (1957) J. Chem. Phys. 27, 1311

Bearden, J.A. and Watts, H.M. (1951) Phys. Rev. 81, 75.

- Beckett, G.W., Freeman, N.K. and Pitzer, K.S. (1948) *J. Amer. Chem. Soc.* 70, 4227.
- Bloch, F., Hansen, W.W. and Packard, M.E. (1946) *Phys. Rev.* 69, 127.
- Bloembergen, N. (1948) *Nuclear Magnetic Relaxation*. The Hague: Nijhoff.
- Bloembergen, N. (1949) *Physica* 15, 386.
- Bloembergen, N., Purcell, E.M. and Pound, R.V. (1948) *Phys. Rev.* 73 679.
- Brockway, L.O. and Robertson, J.M. (1939) *J. Chem. Soc.* 1934.
- Coulson, G.A. and Moffitt, W.E. (1949) *Phil. Mag.* 40, 1.
- Cox, E.G. (1932) *Proc. Roy. Soc.* A135, 491.
- Dicke, R.H. (1946) *Rev. Sci. Inst.* 17, 268.
- Eades, R. G. (1952) Thesis, University of St. Andrews.
- Eyring, H., Walter, J. and Kimball, G.E. (1944) *Quantum Chemistry*. New York: John Wiley & Sons, Inc.
- Flett, M.S.C., Cave, W.T., Vago, E.E. and Thompson, H.W. (1947) *Nature* 159, 739.
- French, F.A. and Rasmussen, R.S. (1946) *J. Chem. Phys.* 14, 389.
- Gorter, G.J. (1936) *Physica* 3, 995.
- Gorter, G.J. and Broer, L.F.J. (1942) *Physica*, 9, 591.
- Gutowsky, H.S. and Pake G.E. (1950) *J. Chem. Phys.* 18, 162.
- Hansen, G.E. and Dennison, D.M. (1952) *J. Chem. Phys.* 20, 313.
- Heitler, W. and Teller, E. (1936) *Proc. Roy. Soc.* A155, 629.

- Herzberg, G. (1945) *Infrared and Raman Spectra of Polyatomic Molecules.*  
New York: D. Van Nostrand Co, Inc.
- Huffman, H.M., Eaton, M. and Oliver, G.D. (1948) *J. Amer. Chem. Soc.*  
70, 2911.
- Huffman, H.M., Parks, G.S. and Bernore, M. (1931) *J. Amer. Chem. Soc.*  
53, 3876.
- International Tables for X-Ray Crystallography.* Edrmingham:  
Kynoch Press.
- Karle, I.L. (1952) *J. Chem. Phys.* 20, 65.
- Kaufman, H.S., Fankuchen, I. and Mark, H. (1947) *J. Chem. Phys.* 15, 414.
- Kaufman, H.S., Fankuchen, I. and Mark, H. (1948) *Nature* 161, 165.
- Kistiakowsky, G.B., Lacher, J.R. and Stitt, F. (1939) *J. Chem. Phys.*  
7, 289.
- Lippincott, E.R. and Lord, R.C., Jr. (1946) *J. Amer. Chem. Soc.* 68, 1868.
- Lippincott, E.R. and Lord, R.C., Jr. (1951) *J. Amer. Chem. Soc.* 73, 3889.
- Lippincott, E.R., Lord, R.C., Jr. and McDonald, R.S. (1948) *J. Chem. Phys.*  
16, 548.
- Lippincott, E.R., Lord, R.C., Jr. and McDonald, R.S. (1950) *Nature* 166,  
227.
- McDonnell, F.R.M., Pink, R.C. and Ubbelohde, A.R. (1950) *Trans. Faraday*  
*Soc.* 46, 156.
- Moxon, L.A. (1949) *Recent Advances in Radio Receivers.* Cambridge  
University Press.
- Müller, A. (1928) *Proc. Roy. Soc. A* 120, 437.
- Müller, A. (1930) *Proc. Roy. Soc. A* 127, 417.

- Müller, A. (1930) Proc. Roy. Soc. A 138, 514.
- Pake, G.E. (1948) J. Chem. Phys. 16, 327.
- Pauli, W. (1924) Naturwissenschaften 12, 741.
- Pauling, L. (1948) The Nature of the Chemical Bond. New York: Cornell University Press.
- Person, W.E., Pimentel, G.C. and Pitzer, K.S. (1952) J. Amer. Chem. Soc. 74, 3437.
- Pink, R.C. and Ubbelohde, A.R. (1948) Trans. Faraday Soc. 14, 708.
- Pitzer, K.S. (1951) Disc. Faraday Soc. 10, 66.
- Round, R.V. (1952) Prog. Nucl. Phys. 2, 21.
- Powles, J.G. and Outowsky, H.S. (1954) J. Chem. Phys. 23, 1692.
- Prosen, E.J., Johnson, W.H. and Rossini, F.D. (1947) J. Amer. Chem. Soc. 69, 2068.
- Purcell, E.M., Torrey, H.G. and Pound, R.V. (1946) Phys. Rev. 69, 37.
- Rabi, I.I., Millman, S., Kusch, P. and Zacharias, J.R. (1939) Phys. Rev. 55, 526.
- Rollin, B.V. and Hatton, J. (1948) Phys. Rev. 74, 346.
- Rushworth, F.A. (1952) J. Chem. Phys. 20, 920.
- Rushworth, F.A. (1953) Thesis, University of St. Andrews.
- Rushworth, F.A. (1954) Proc. Roy. Soc. A 222, 526.
- Saksena, B.D. and Bhatnagar, S.S. (1953) Current Science 22, 138.
- Saksena, B.D. and Narain, H. (1950) Nature 165, 723.



- Scott, D.W., Gross, M.E., Oliver, G.D. and Huffman, H.M. (1949)  
*J. Amer. Chem. Soc.* 71, 1634.
- Spangenberg, K.R. (1948) *Vacuum Tubes*. New York: McGraw-Hill Inc.
- Timmermans, J. (1950) *Physico-Chemical Constants of Pure Organic Compounds*. Amsterdam: Elsevier.
- Van Vleck, J.H. (1948) *Phys. Rev.* 74, 1168.
- Waller, I. (1932) *Z. Phys.* 79, 370.
- Walkman, H. MacNee, A.B. and Gadsden, G.P. (1948) *Proc. I.R.E.* 36, 700.